IDENTIFICATION OF NOVEL SUBSTRATES FOR AURKA AND LIMK2

by

Hanan Haymour

A Dissertation

Submitted to the Faculty of Purdue University

In Partial Fulfillment of the Requirements for the degree of

Doctor of Philosophy

Department of Chemistry

West Lafayette, Indiana

May 2019

THE PURDUE UNIVERSITY GRADUATE SCHOOL
STATEMENT OF COMMITTEE APPROVAL

Dr. Kavita Shah, Chair
Department of Chemistry
Dr. Philip Low
Department of Chemistry
Dr. Alexander Wei
Department of Chemistry
Dr. Chittaranjan Das
Department of Chemistry

Approved by:

Dr. Christine Hrycyna
Head of the Graduate Program

Dedicated to the memory of my father

ACKNOWLEDGMENTS

The graduate school experience is a long journey, and although all students go through the same process, this journey has many paths to the same destination. I can say that my journey was unusual in nature, and I would like to express my gratitude to the people who made this journey a special one, with both its good and tough times.

I would like to sincerely thank and extend my appreciation to the many people who helped me throughout the years of graduate school.

Starting with my committee chair, Professor Kavita Shah. Dr. Shah provided guidance and support to help me complete my work in a shorter period, compared to the time usually required from students to finish their degree. I learned from Dr. Shah many lessons on how to conduct academic research. I was grateful for the chance to work in her research group four years into my graduate school journey. I learned so much about our field of research in her lab, which was different from the field I started my graduate studies in. Dr. Shah was always available whenever we needed advice, she knew the specific details of our work and gave detailed guidance whenever required. I will never forget the lessons I learned as her student.

I also would like to thank Professor Philip Low from my research committee, who guided me through research in the early stages of my degree for almost four years. Although this dissertation does not cover the work I did in his laboratory, I learned from him how to be independent and take initiative, how to organize my research and be critical in my thinking. I learned from him the importance of reading about what we do in lab in order to have a better understanding of the work we do.

I would like to thank Professor Alex Wei, also from my research committee, whom I highly respect. Although our collaboration projects did not continue, Dr. Wei provided me with the initial guidance in my graduate school experience. I am also thankful to Professor Chittaranjan Das for accepting to be the fourth committee member on my final defense exam, and for the time and effort he is investing in me.

I would like to deeply thank Dr. Nikhil Kumar from our research group, who was the second person after Dr. Shah to provide me with great help. His initial results are what

opened the door for this research. I would like to thank him for providing all the kinases for everyone in our research group. His assistance is greatly appreciated.

I would like to thank my research group members, Dr. Keith Viccaro, who graduated last year from our lab, as he was the first person to teach me some of the techniques I needed for the success of my experiments. I would also like to thank Benjamin Ramsey for his willingness to help in the LIMK2/YBX1 project. Finally, I would like to thank Asif Raza and Hyunjin Kim for their support, as well as all the undergraduate students who worked in our lab in general, particularly Jiachong Chu and Benjamin Flueckiger for helping in protein expression, purification and other side lab-work.

Special thanks to the people in Professor Christine Hrycyna's research group who provided the development machine, and for their welcoming environment while we used their lab for our experiments. And special thanks to professor Das's group for kindly providing us with two samples of competent cells to grow and make our own.

Special thanks, also, to all the people in the Chemistry Department who helped us throughout graduate school. I am thankful to the people who helped me with the final editing of this dissertation, Dr. Nikhil Kumar, Fatima Hasabelnaby and Ahmad Gheith.

I am very grateful to my husband, Ahmad Gheith, for his moral and financial support. Without him, I would not be able to be here today. I dedicate this thesis to him, and to my family and friends whose love and encouragement provided me with the energy to continue my work. I am particularly grateful to my mother, who always reminded me that no one can take away my hard work and sincerity, and to my late father, who taught me to love science and to see it as a means towards a better world.

Once again, I thank you all.

This work was supported by the NIH and DoD

TABLE OF CONTENTS

TABLE OF CONTENTS 6
LIST OF TABLES 10
LIST OF FIGURES 11
ABSTRACT 17
CHAPTER 1. INTRODUCTION 19
1.1 Prostate Cancer 19
1.2 LIM Kinase 2 (LIMK2) 20
1.2.1 LIMK2 structure and domain 20
1.2.2 LIMK2 function, activation, and regulation 21
1.2.3 LIMK2 in cancer 21
1.3 Aurora A kinase (AURKA) 22
1.3.1 AURKA structure and domain 22
1.3.2 AURKA function in normal cells 23
1.3.3 AURKA in cancer 26
1.3.4 AURKA in CRPC 26
1.4 Speckle-type POZ protein (SPOP) 26
1.4.1 Nuclear and nuclear speckle protein 26
1.4.2 SPOP Function 27
1.4.3 SPOP Domains 28
1.4.4 SPOP in Cancer 29
1.4.5 SPOP in Prostate Cancer 30
1.5 Y-box binding protein (YBX1) 31
1.5.1 YBX1 structure and function 31
1.5.2 YBX1 in cancer 32
1.5.3 YBX1 in prostate cancer 33
1.6 References 34
CHAPTER 2. SPOP IS A DIRECT SUBSTRATE FOR LIMK2 45
2.1 Introduction 45
2.2 Results 46

2.2.1 LIMK2 regulates SPOP at the protein expression level 46
2.2.2 SPOP alteration of LIMK2 protein expression level 46
2.2.3 LIMK2 directly phosphorylates SPOP 48
2.2.4 SPOP Fragmentation 49
2.2.5 Phosphorylation of SPOP on S59A, S171A, and S226A 52
2.3 Discussion 56
2.4 Material and Methods 57
2.4.1 Buffers 57
2.4.2 PCR Primers 57
2.4.3 SPOP Fragmentation 57
2.4.4 Cloning and Site-Directed Mutagenesis 58
2.4.5 Transformation and production of plasmid DNA 58
2.4.6 Bacterial Protein Expression and purification 58
2.5 References 58
CHAPTER 3. SPOP IS A DIRECT SUBSTRATE FOR AURKA 61
3.1 Introduction 61
3.2 Results 61
3.2.1 AURKA and SPOP regulation relationship 61
3.2.2 AURKA binds SPOP associates with each other 62
3.2.3 AURKA directly phosphorylates SPOP 63
3.2.3.1 Predicting SPOP phosphorylation sites by Aurora A kinase 64
3.2.3.2 Aurora A phosphorylates SPOP-MATH Domain 64
3.3 Discussion 68
3.4 Material and Methods 69
3.4.1 Buffers 69
3.4.2 PCR Primers 69
3.4.3 Cloning and Site-Directed Mutagenesis 70
3.4.4 Transformation and production of plasmid DNA 70
3.4.5 Bacterial Protein Expression and purification 70
3.4.6 Sf9 cell protein expression and purification 70
3.5 References 70

CHAPTER 4. YBX1 IS A DIRECT SUBSTRATE OF AURKA 72
4.1 Introduction 72
4.2 Results 73
4.2.1 Aurora A kinase regulates YBX1 at the protein expression level 73
4.2.2 AURKA and YBX1 associate with each other 74
4.2.3 YBX1 is directly phosphorylated by AURKA 74
4.2.3.1 Predicting YBX1 phosphorylation sites by Aurora A kinase 75
4.2.4 Aurora A phosphorylates YBX1 on T62A, S102A sites 76
4.3 Material and Methods 79
4.3.1 Cloning and site-directed mutagenesis 79
4.3.2 PCR primers 79
4.3.3 Transformation and production of plasmid DNA 79
4.3.4 Bacterial protein expression and purification 79
4.3.5 Buffers 79
4.4 References 80
CHAPTER 5. METHODOLOGY 82
5.1 Cloning and Site-Directed Mutagenesis 82
5.2 Competent cells preparation 84
5.3 Sf9 cell protein expression and purification 84
5.4 Transformation and production of plasmid DNA 84
5.5 Bacterial 6-His-tagged Protein Expression 85
5.6 Bacterial 6-His-tagged protein purification 86
5.7 Peptide Assay 87
5.8 Kinase Assays 87
1.8.1 Preparing and purifying the kinase 87
5.8.1 Cold ATP reaction 88
5.8.2 Sample preparation 88
5.9 Buffers and solution recipes 90
5.9.1 Buffers for purifying plasmid DNA 90
5.9.2 Buffers for DNA agarose gel 90
5.9.3 Buffers for Protein Purification 90

5.9.4 Buffers for western blot and protein staining 91

LIST OF TABLES

Table 5.1: List of SPOP primers 83
Table 5.2: List of YBX1 primers 84
Table 5.3: General sample preparation for kinase assay 89

LIST OF FIGURES

Figure 1.1 LIMK2 structure and domains. LIMK2 is similar to LIMK1 in having two unique N-terminal LIM domains, a PDZ domain and proline/serine (P/S) rich domain, and finally the C-terminal kinase domain..... 20

Figure 1.2 AURKA structure and domains. AURKA contains three putative conserved Aurora boxes (pink) at the N-terminal domain, a kinase domain (also called the catalytic domain), and a c-terminal domain. (dark blue) Destruction-box (D-box) is a short amino-acid motif in the C-terminal region that is recognized by the multi-subunit E3-ubiquitin ligase anaphase, and functions in promoting complex/cyclosome (APC/C) for ubiquitination and proteasomal degradation[2], while the N-terminal region is involved in protein-protein interaction. AURKA's regulation occurs by phosphorylation on a conserved residue, threonine 288 (yellow), which increases the AURKA enzymatic activity. 23

Figure 1.3 Role of AURKA in mitosis. When AURKA is activated after Thr288 auto-phosphorylation, Bora is then phosphorylated by AURKA, which further enhances AURKA activity. AURKA then activates CDK1-Cyclin B by phosphorylation to allow activation of G2/M checkpoint mechanisms, such as PLK1-dependent targeting of Wee1 and CDC25C. What follows is CDC25B-dependent activation of CDK1, and finally, direct phosphorylation of CDK1. Additionally, PLK1 mediates Bora degradation to allow mitosis progression. At G2/M, AURKA localizes in the centrosome, and also contributes to their maturation before mitotic entry. At prophase, Ajuba maintains AURKA activity, which in turn recruits and phosphorylates several PCM proteins to organize the MTOC. At metaphase, AURKA moves to the proximal MT and targets MT-associated proteins and organizes the mitotic spindle. In this stage, TPX2 mediate the activity of AURKA. 25

Figure 1.4 SPOP as a substrate adapter for CUL3-based ubiquitin ligases (CRL3): the SPOP-BTB domain assembles with CUL3, building the ubiquitin ligase complex and making a two-substrate binding site that will lead to ubiquitination and protein degradation.

Mutations in the MATH domain prevent SPOP binding with SRC-3 protein and cannot promote its degradation..... 28

Figure 1.5 Schematic overview of the SPOP gene and sites of mutation in prostate cancer. All SPOP mutation sites in prostate cancer are clustering in the MATH domain. Mutant SPOP cannot bind to its substrates or cause their degradation..... 29

Figure 1.6 The proposed mechanism of SPOP binding to its substrate. (A) Illustrates the substrate binding to wild-SPOP, inducing protein ubiquitination. (B) The inability of the substrate to bind to mutated SPOP. (C) The mutated substrate is not binding to wild-type SPOP, (SPOP domains are shown in blue: MATH domain, Red: BTB domain, and green: BACK domain). 30

Figure 1.7 Schematic diagram of YBX-1 protein structure, functions and possible therapeutic strategies. The C-terminal domain of YB-1 consists of four alternating clusters of basic and acidic amino acids. YBX-1 is acting both as a transcription and translation factor. Along with being involved directly in pre-mRNA splicing, mRNA translation and DNA replication and repair, YBX-1 can affect many pro-tumorigenic events (light-blue boxes) participating in cancer progression. Possible therapeutic strategies are presented (purple color) 34

Figure 2.1 LIMK2 regulates SPOP protein level. (A) LIMK2 overexpression in C4-2 cells reduces the SPOP protein expression level. (B) The removal of LIMK2 using LIMK2-shRNA1 and LIMK2-shRNA2 elevates SPOP protein levels in C4-2 cells compared to control cells. (C) LIMK2 overexpression and LIMK2-removal are together compared to control cells. (D) LIMK2 overexpression in 22Rv1 cells decreases the SPOP protein expression level. (E) LIMK2 removal using LIMK2-shRNA1 and LIMK2-shRNA2 increases SPOP protein levels in 22Rv1 cells compared to control cells. (F) LIMK2 overexpression and LIMK2 removal in 22Rv1 cells is compared to control cells 47

Figure 2.2 LIMK2 directly phosphorylates WT-SPOP. The first lane from the left is LIMK2 alone, the second lane is WT-SPOP with LIMK2, and the third lane is SPOP alone.

All samples have a 10X kinase buffer, 0.5 μCi [γ-32P] ATP and DI-H_2O to adjust the reaction to a 25μL final scale. 48

Figure 2.3 A crystallized structure of SPOP illustrates its fragmentation into three pieces: (Blue) SPOP-1-180 which contains the MATH domain, SPOP-1-180 was cloned into the TAT-HA vector at the BamHI and EcoRI sites; (Red) SPOP-181-300 which contains the BTB domain in SPOP, was cloned into the TAT-HA vector at the BamHI and XhoI sites; and (Green, the smaller piece in the figure) SPOP-301-374 in the C-terminus domain region, was cloned into the TAT-HA vector at the BamHI and XhoI sites. All SPOP-fragments are 6x-His tagged. 50

Figure 2.4 LIMK2 phosphorylates SPOP-1-180 and SPOP-181-300. The 1st line (L1) from the left is LIMK2 alone. (L2) is SPOP-1-180 with LIMK2, and (L3) is SPOP-1-180 alone. (L4) shows SPOP-180-300 with LIMK2, (L5) is SPOP-180-300 alone. (L6) is SPOP-301-374 with LIMK2, and (L7) SPOP-301-374 is alone. All samples have a 10X kinase buffer, 0.5 μCi [γ-32P] ATP and DI-H_2O to adjust the reaction to a 25μL final scale 51

Figure 2.5 The identification of SPOP phosphorylation sites by LIMK2. (A) A crystal structure of SPOP illustrates the identified phosphorylation sites Ser59, Ser171 and Ser226, and their localization in these domains: the (Blue) SPOP-MATH domain, and (Red) SPOP-BTB domain. (B) The amino-acid residue sequence showing the SPOP-sites of phosphorylation by LIMK2 favoring a glycine or alanine followed the phosphorylation sites. (C) A representation of the SPOP structural domains, showing the SPOP phosphorylation sites by LIMK2 and its localization. P1, P2, and P3 are the original fragments generated to predict the phosphorylation sites. 53

Figure 2.6 Phosphorylation reduction in SPOP mutants compared to WT-SPOP. LIMK2 phosphorylates SPOP at S59, S171, and S226. Lane 1 (L1) contains LIMK2 only(L2) contains WT-SPOP and LIMK2, (L3) contains SPOP-S59A mutant and LIMK2, (L4) contains SPOP-S171A mutant and LIMK2, (L5) contains SPOP-S226A mutant and LIMK2. All lanes also have, [^{32}P]ATP, 10X kinase buffer and DI-H_2O to adjust the reaction to 25μL final scale. Also, all SPOPs are 6x-His tagged. Kinase assay was conducted for 30

min. The Top panel shows autoradiography and the bottom panel shows LIMK2 and SPOPs coomassie blue stain. The mutants were generated and subjected to *in vitro* kinase assay using LIMK2. The bar graph shows the phosphor-resistant mutants of SPOP compare to WT-SPOP 54

Figure 2.7 LIMK2 directly phosphorylates SPOP. (A) The top panel shows autoradiography and the bottom panel shows LIMK2 and SPOP's Coomassie blue stain. LIMK2 phosphorylates SPOP at S59, S171, and S226 (S226 is not shown in this experiment). Lane 1 (L1) contains SPOP-S171A mutant and LIMK2, (L2) contains SPOP-S59A mutant and LIMK2, (L3) contains WT-SPOP and LIMK2, (L4) contains LIMK2 only, (L5) contains WT-SPOP and LIMK2, (L6) contains SPOP-S171A mutant and LIMK2, (L7) contains SPOP-S59A mutant and LIMK2, (L8) contains SPOP-S171A mutant and LIMK2, (L9) contains SPOP-S59A mutant and LIMK2, (L10) contains WT-SPOP and LIMK2, (L11) contains LIMK2 only, (L12) contains WT-SPOP and LIMK2, (L13) contains SPOP-S171A mutant and LIMK2, (L14) contains SPOP-S59A mutant and LIMK2. All samples also have a [^{32}P]ATP, 10X kinase buffer. All SPOPs are 6x-His tagged. A kinase assay was conducted for 30 min. The mutants were generated and subjected to the *in vitro* kinase assay using LIMK2. (B) A bar graph shows the phosphor-resistant mutants of SPOP compare to WT-SPOP in four sets of experiments. (C) (L1) contains LIMK2 only, (L2) contains the SPOP-3M (S59A, S171A, and S226A) mutant and LIMK2, (L3) contains WT-SPOP and LIMK2. All lanes also contain a [^{32}P]ATP, 10X kinase buffer..... 55

Figure 3.1 AURKA directly phosphorylates WT-SPOP. The first lane is AURKA alone, the second lane is WT-SPOP with AURKA, and the third lane is SPOP alone. All samples have a 10X kinase buffer, 0.5 μCi [γ-32P] ATP and DI-H2O to adjust the reaction to a 25μL final scale. 63

Figure 3.2 SPOP phosphorylation sites by AURKA are clustered in the MATH domain. AURKA directly phosphorylates SPOP at the sites Ser33, Thr56 and Ser105, and all sites localizae in the MATH domain**.** The phosphorylated sites are marked in yellow color. 65

Figure 3.3 Phosphorylation reduction in SPOP mutants compared to WT-SPOP. AURKA phosphorylates SPOP at S33, T56, and S105. (A) Lane 1 (L1) contains AURKA only, (L2) contains WT-SPOP and AURKA, (L3) contains the SPOP-S33A mutant and AURKA, (L4) contains the SPOP-T56A mutant and AURKA, (L5) contains the SPOP-S105A mutant and AURKA. All lanes also contain a [^{32}P]ATP, 10X kinase buffer and DI-H_2O to adjust the reaction to a 25µL final scale. Noted also, all SPOPs are 6x-His tagged. A kinase assay was conducted for 30 min. (B) (L1) contains AURKA only, (L2) contains WT-SPOP and AURKA, (L3) contains the SPOP-3M (S33A, T56A, and S105) mutant and AURKA. All lanes also contain a [^{32}P]ATP, 10X kinase buffer and DI-H_2O to adjust the reaction to a 25µL final scale. All SPOPs are 6x-His tagged. A kinase assay was conducted for 30 min.(C) Bar graph shows the phosphor-resistant individual mutants of SPOP compared to WT-SPOP..... 66

Figure 3.4 The identification of SPOP phosphorylation sites by AURKA. (Left side) a crystal structure of SPOP illustrates the identified phosphorylation sites Ser33, Thr56 and Ser105, and their localization in the MATH domain. (Right side) is the amino-acid sequence recognized by AURKA, where the residue following the site of phosphorylation is hydrophobic. The phosphorylation sites of SPOP by AURKA are circled. 67

Figure 4.1 YBX1 structure and domains. YBX1 contains aniline/proline rich N-terminal domain, the cold shock domain CSD, and the C-terminal tail domain. Serine 102 (S102) is the first phosphorylation site identified for YBX1 in the CSD region. 73

Figure 4.2 AURKA directly phosphorylates WT-YBX1. The first lane is AURKA alone, the second lane is WT-YBX1 with AURKA, and the third lane is YBX1 alone. All samples have a 10X kinase buffer, 0.5 µCi [γ-32P] ATP and DI-H2O to adjust the reaction to a 25µL final scale. 75

Figure 4.3 Phosphorylation reduction in YBX1 mutants compared to WT-YBX1. AURKA phosphorylates YBX1 at S62 and S102. (A) Lane 1 (L1) contains AURKA only, (L2) contains WT-YBX1 and AURKA, (L3) contains the YBX1-S62A mutant and AURKA, (L4) contains the YBX1-S102A mutant and AURKA, (L5) contains WT-YBX1 only, (L6) contains YBX1-S62A only, and (L7) contains YBX1-S102A only. All lanes also

contain a [^{32}P]ATP, 10X kinase buffer and DI-H_2O to adjust the reaction to a 25µL final scale. Noted also, all YBXs are 6x-His tagged. A kinase assay was conducted for 30 min. (B) (L1) contains AURKA only, (L2) contains WT-YBX1 and AURKA, (L3) contains the YBX1-2A (S62A and S102A) mutant and AURKA. All lanes also contain a [^{32}P]ATP, 10X kinase buffer and DI-H_2O to adjust the reaction to a 25µL final scale. All SPOPs are 6x-His tagged. A kinase assay was conducted for 30 min. (C) Bar graph shows the phospho-levels of WT and phospho-resistant single mutant of YBX1 (D) Bar graph shows that the phospho-levels of WT and phospho-resistant double mutant (S62 and S102) of YBX1. 77

Figure 4.4 The identification of YBX1 phosphorylation sites by AURKA. (Top) A crystal structure of the YBX1-CSD domain illustrates the identified phosphorylation sites Ser62 and Ser102, as well as their localization in the CSD domain. (Right side) is the amino-acid sequence recognized by AURKA, where the residue following the site of phosphorylation is hydrophobic. The phosphorylation sites of YBX1 by AURKA are circled..... 78

Figure 5.1 Step flow-chart overview of cloning and site directed mutagenesis...... 82

ABSTRACT

Author: Haymour, Hanan, S. PhD
Institution: Purdue University
Degree Received: May 2019
Title: Identification of Novel Substrates for AURKA and LIMK2
Committee Chair: Kavita Shah

LIMK2 is a serine/threonine/tyrosine kinase that promotes tumor cell invasion and metastasis by phosphorylating cell proteins and altering their functions. There is a need to find tumor-specific substrates for LIMK2 in order to understand the downstream pathway of these substrates, their function, and how they are regulated by LIMK2. Recently, our labrotory identified LIMK2 as an excellent target for curing castration-resistant prostate cancer (CRPC). In this study, we identify two novel substrates for LIMK2 in CRPC: speckle-type POZ protein (SPOP), and Y-box binding protein-1 (YBX1). While LIMK2 negatively regulates SPOP, it positively regulates YBX1 − both by phosphorylation using *in-vitro* kinase assays. A study in our labrotory also proved that LIMK2 regulates Aurora A kinase (AURKA), where AURKA directly phosphorylates LIMK2. AURKA is a serine/threonine kinase that regulates cell cycle during mitosis; it is known to be up-regulated, with uncontrolled activity, in many types of cancer, including prostate cancer. It is therefore important to identify new substrates for AURKA, especially in light of reported lethality in early embryonic mice, in association with AURKA-knockout. In other words, targeting AURKA directly may cause severe toxicity, a finding that has prevented direct inhibitors from passing Phase II clinical trials. In this study, we also identified SPOP and YBX1 as direct substrates for AURKA. Our results confirm what we know about the LIMK2/AURKA relationship: that AURKA negatively regulates SPOP and positively

regulates YBX1. Targeting LIMK2 and AURKA indirectly through SPOP, YBX1 and its other substrates holds tremendous therapeutic potential in treating prostate cancer. With this, we open the door for researches to investigate the direct phosphorylation of SPOP and YBX1 in other types of cancer cells known to have overexpression in SPOP and/or YBX1.

CHAPTER 1. INTRODUCTION

1.1 Prostate Cancer

Prostate Cancer (PCa) is known to be the most common type of cancer in men worldwide, and the second death-causing cancer in the US[1,3]. Early stages of PCa can be treated by androgen-deprivation therapy (ADT)[1]. In aggressive PCa, the options include radiation therapy, surgery and brachytherapy[4]. Although available therapies have significantly improved survival rates, almost all patients relapse within several years due to reactivation of androgen receptor (AR) signaling pathways; and despite the testosterone levels present in these patients, the PCa becomes more aggressive and at this stage is called castration-resistant prostate cancer (CRPC)[1, 5].

Multiple pathways show genomic alterations in PCa, including the androgen receptor signaling pathway; the phosphoinositide 3-kinase (PI3K) pathway; loss of function of the prostate tumor suppressor genes, such as NKX3.1; and the up-regulation/down-regulation of transmembrane serine protease 2 (TMPRSS2), which captivate the ETS transcription factors family by way of the androgen responsive promotor[6].

Mutation in the tumor suppressor gene, PTEN, has been found to be connected to PCa progression by activation of PI3K/AKT pathways[7]. Other mutations in several genes have been identified as well, including DICER, HDAC9, CHD5, CHD1, ZNF407, SPTA1 and SPOP[7].

PCa cells develop different mechanisms to overcome the hormonal stress of ADT and become resistant to therapy after some time. Investigating the CRPC cells' mechanisms

at the molecular and genetic level as compared to the PCa cells in early stages is necessary to provide new approaches to treat CRPC[8].

1.2 LIM Kinase 2 (LIMK2)

1.2.1 LIMK2 structure and domain

LIM Kinase 2 (LIMK2) is a member of the LIM kinase (LIMK) family[9, 10]. LIMK2 is a serine/threonine, and sometimes a tyrosine kinase. LIMK2 is highly expressed in the brain, kidney, lung, stomach, and testis[9]. LIMK2 is encoded by different genes located on human chromosomes 22q12.2. This kinase, just like LIMK1, has a unique two N-terminal LIM domains and a C-terminal kinase domain, in addition to a PDZ and proline/serine (P/S) rich domains[10, 11] (Figure 1.1). The LIM domains regulate the kinase activity[12] and have been shown to be involved in protein-protein interactions, and possibly in protein-DNA interactions[9, 12-14]. Although LIMK2 is localized mainly in the cytoplasm[10], LIMK2 subcellular location can be influenced by the PDZ domain that mediates a protein-protein interaction regulating the nuclear/cytoplasmic shuttling processes using two leucine-rich nuclear export signals[15, 16]. Specific nuclear signals found in the domains drive LIMK1 and LIMK2 kinases translocation-process into the nucleus[17].

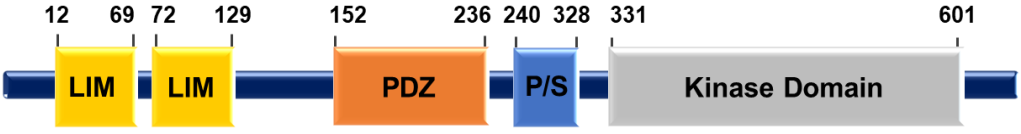

Figure 1.1 LIMK2 structure and domains. LIMK2 is similar to LIMK1 in having two unique N-terminal LIM domains, a PDZ domain and proline/serine (P/S) rich domain, and finally the C-terminal kinase domain.

1.2.2 LIMK2 function, activation, and regulation

LIM and PDZ domains have been shown to regulate LIMK2 activity. The activity of LIMK2 kinase increases by deletion or mutation of LIM-cysteine residues[12]. Furthermore, the activity increases by mutation or deletion of both LIM and PDZ domains together[9, 12]. Phosphorylation is one of the other factors that can affect LIMK2 activity. For example, LIMK2 phosphorylation at threonine-505 by Rho-associated protein kinase (ROCK), is essential for initial LIMK2 activation[18]. LIMK2 activation of phosphorylation by the myotonic dystrophy kinase-related Cdc42-binding kinase has also been reported[19]. While phosphorylating LIMK2 in the kinase domain increases its activity, phosphorylation outside the kinase domain is associated with shuttling of LIMK2 to and from the nucleus interfering with its function. For example, the protein kinase C (PKC) has been reported to phosphorylate LIMK2 at serine 283 and threonine 494 residues, inhibiting its nuclear import in endothelial cells[20]. Another study from our laboratory identified Aurora A kinase (AURKA) as a regulator for LIMK2, engaging in a positive feedback loop and suggesting LIMK2 as a substrate for AURKA by phosphorylation in breast cancer cells[21].

The LIM kinase family are well known as regulators of actin cytoskeletal dynamics, mediating the regulation of cell morphology and motility[9, 10]. The most studied substrate for LIMK1 and LIMK2 is cofilin, where it has been shown that the LIMK2-Rho-Cdc42 pathway mediates the regulation of actin dynamics by phosphorylating cofilin[9, 21, 22].

1.2.3 LIMK2 in cancer

The LIM kinases have been proposed to play an essential role in tumor-cell invasion and metastasis since LIMK2 is also associated with the actin cytoskeleton, with cell shape, and

with motility mechanisms[23]. It was also proposed that the ratio between phosphorylated and dephosphorylated cofilin has a significant impact on tumor aggressiveness and tumor-cell invasion[9]. Many reports have shown LIMK2 upregulation in several types of cancer[24-28]. A recent study from our laboratory identified LIMK2 upregulation in Prostate cancer upon castration in both mice and human CRPC tissues. Most importantly, inducible knockdown of LIMK2 fully reversed tumorigenesis in mouse models, identifying LIMK2 as a potential therapeutic target for CRPC[28]. To date, the molecular mechanisms by which LIMK2 promotes tumorigenesis, angiogenesis, chemoresistance, and invasion remain unknown. Identification of direct substrates of LIMK2 are expected to uncover the molecular mechanisms of LIMK2-induced oncogenesis.

1.3 Aurora A kinase (AURKA)

1.3.1 AURKA structure and domain

Aurora A kinase (AURKA) is a highly conserved serine/threonine kinase that is expressed in most cell types, and it is essential for cell survival. AURKA is mainly expressed during G2 and M phases of the cell cycle and localizes to the duplicated centrosomes starting from the S phase. It then shifts to the bipolar spindle microtubules during mitosis to regulate chromosomal alignment and separation during those phases.[29] In mammals, the Aurora kinase family consists of AURKA, AURKB, and AURKC. Our focus is on AURKA only. AURKA contains an N-terminal domain, a kinase domain, and a c-terminal domain (Figure 1.2). The protein kinase domain, including the destruction-box (D-box), is common in all of the AURK family[2]. The D-box is a short amino-acid motif in the C-terminal region that is recognized by the multi-subunit E3-ubiquitin ligase anaphase, and functions in

promoting complex/cyclosome (APC/C) for ubiquitination and proteasomal degradation[2], while the N-terminal region is involved in protein-protein interaction[30].

Figure 1.2 AURKA structure and domains. AURKA contains three putative conserved Aurora boxes (pink) at the N-terminal domain, a kinase domain (also called the catalytic domain), and a c-terminal domain. (dark blue) Destruction-box (D-box) is a short amino-acid motif in the C-terminal region that is recognized by the multi-subunit E3-ubiquitin ligase anaphase, and functions in promoting complex/cyclosome (APC/C) for ubiquitination and proteasomal degradation[2], while the N-terminal region is involved in protein-protein interaction. AURKA's regulation occurs by phosphorylation on a conserved residue, threonine 288 (yellow), which increases the AURKA enzymatic activity.

1.3.2 AURKA function in normal cells

In the cell cycle, AURKA is rarely detectable during the G1 phase and slightly detectable in the S phase at the centrosome. AURKA accumulates at the centrosome and becomes active during the late G2 phase[30]. Activated AURKA is found on the bipolar spindles and spindle poles during the prometaphase and the metaphase. After that, most of AURKA becomes inactivated in the following phase[30].

In normal cells, AURKA is required for centrosome duplication, separation, and maturation, as well as mitosis entry, and the formation of the mitotic spindle and cytokinesis[30]. AURKA-induced centrosomal microtubule stabilization through phosphorylation of Transforming acidic coiled-coil protein (TACC)[31]. AURKA can be activated by several co-factors, such as AJUBA, TPX2 (Targeting protein for Xenopus kinesin-like protein 2), TACC, Bora (Protein-aurora-borealis), and via auto-phosphorylation at Threonine288[2]. In the mitotic entry, AURKA couples with Bora, and mediates its activation by phosphorylation of polo-like kinase 1 (PLK1), causing the

activation of Cyclin-dependent kinase 1/cyclin B (CDK1/cyclin B). This occurs by degrading a G2-checkpoint kinase, called Wee1, and activating phosphatase cell division cycle 25C (CDC25C)[31]. CDC25C is also a CDK activator that is phosphorylated by AURKA, and is involved in the G2/M phases transition event[30]. AJUBA Lim-protein activates AURKA at the centrosome, increasing its activity, stimulating the separation of the duplicated centrosomes at G2/M, and initiating the mitotic entry[2, 32]. (Figure 1.3, adapted from [2] and [33]) Deletion of the AURKA gene was found to cause failure in mitotic spindle assembly and chromosomal segregation.

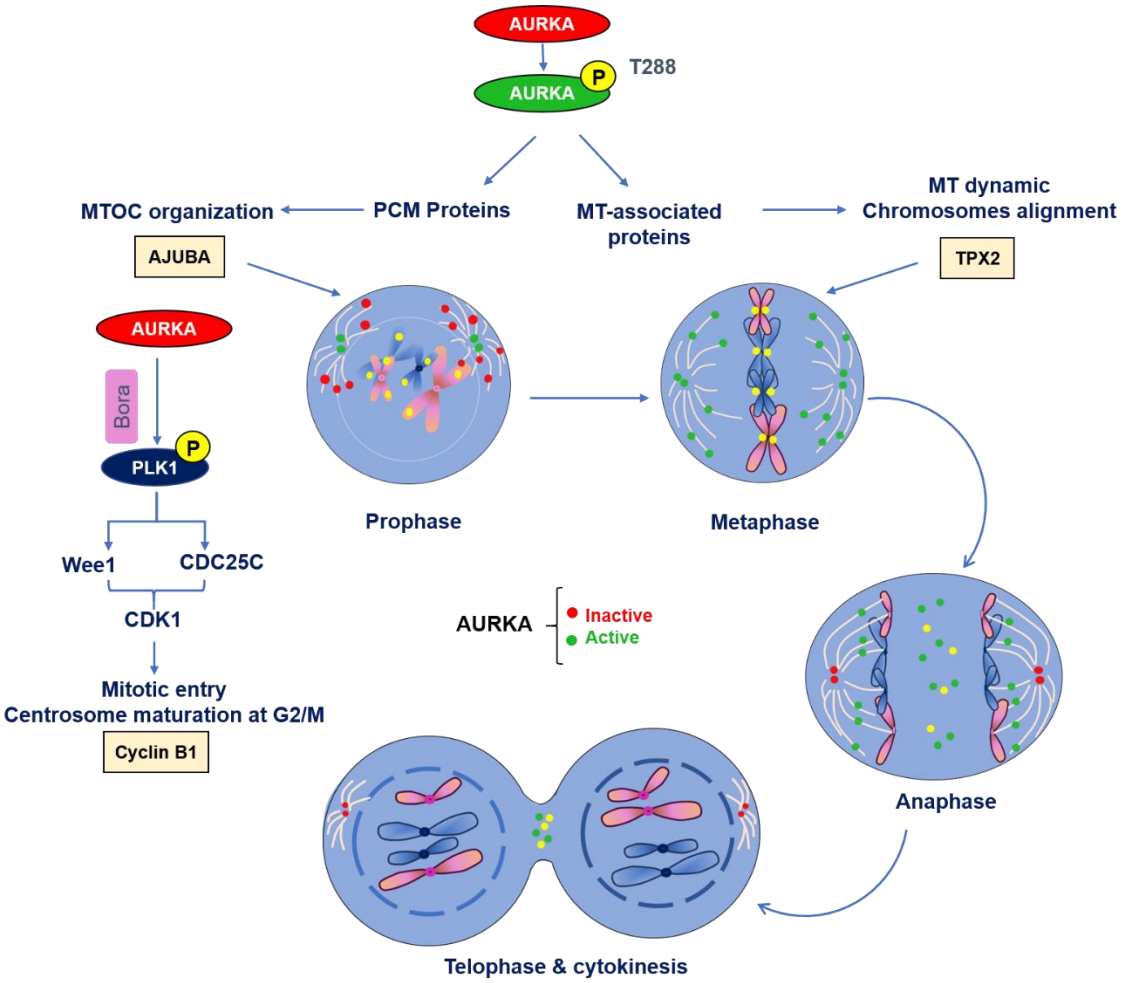

Figure 1.3 Role of AURKA in mitosis. When AURKA is activated after Thr288 auto-phosphorylation, Bora is then phosphorylated by AURKA, which further enhances AURKA activity. AURKA then activates CDK1-Cyclin B by phosphorylation to allow activation of G2/M checkpoint mechanisms, such as PLK1-dependent targeting of Wee1 and CDC25C. What follows is CDC25B-dependent activation of CDK1, and finally, direct phosphorylation of CDK1. Additionally, PLK1 mediates Bora degradation to allow mitosis progression. At G2/M, AURKA localizes in the centrosome, and also contributes to their maturation before mitotic entry. At prophase, Ajuba maintains AURKA activity, which in turn recruits and phosphorylates several PCM proteins to organize the MTOC. At metaphase, AURKA moves to the proximal MT and targets MT-associated proteins and organizes the mitotic spindle. In this stage, TPX2 mediate the activity of AURKA.

1.3.3 AURKA in cancer

AURKA overexpression has been reported in many types of cancer including breast cancer[34, 35], ovarian cancer[36], gastric/gastrointestinal cancer[37], colorectal cancer[38, 39], esophageal squamous cell carcinoma[40], lung cancer[41], cervical cancer[42], prostate cancer[43, 44], glioma[45], acute myeloid leukemia (AML)[46] and oral cancer[47],[33]. AURKA can play critical roles in regulating cancer cells by supporting cell cycle progression and development. Thus, it is not surprising that AURKA functions as an oncogene when overexpressed and promotes tumorigenesis[30, 33]. Importantly, lethality in early embryonic mice was reported in AURKA-knockout mice[48].

1.3.4 AURKA in CRPC

AURKA is upregulated in prostate cancer including in CRPC[43, 49, 50]. Chromatin immunoprecipitation sequencing studies have shown a putative androgen receptor binding site (ARBS) in the promoter and the intron region of AURKA[43, 51, 52]. These studies introduced the AURKA-androgen receptor (AR) binding event as it specifically relates to prostate cancer. Other studies identified the overexpression of the oncogenic transcriptional factor N-Myc and AURKA in metastatic prostate cancer and CRPC, showing that AURKA stabilizes N-Myc and prevents its degradation[53].

1.4 Speckle-type POZ protein (SPOP)

1.4.1 Nuclear and nuclear speckle protein

Speckle-type POZ protein (SPOP) is located in the nucleus and in nuclear speckles[54]. Nuclear speckles are also called splicing factor (SF) compartments, and are identified as small, subnuclear organelles, or as structures that lack membranes (membrane-less). Speckle

proteins are known to participate in the process of transcription and pre-mRNA. 25-50 speckles are observed per mammalian nucleus, and they vary in their shapes and sizes. Depending on the mRNA transcription and regulation, such as phosphorylation of specific proteins, speckles proteins and the RNA-protein components can change their location and may remain in continuous movement[55-57]. A nuclear localization signal (NLS) within SPOP was found to be responsible for nuclear translocation events when engineered intracellular antibodies were bound to the SPOP complex with E3 Ubiquitin ligase, showing that the targeted protein was translocated to the nucleus[58].

1.4.2 SPOP Function

SPOP was discovered in 1997 and identified as nuclear Speckle-type POZ protein[54]. Later, it was discovered that SPOP domains serve as an adaptor of an important multifunctional protein, namely the death domain-associated protein, Daxx, for the ubiquitination by Cul3-based ubiquitin ligase and the degradation by proteasome[59]. SPOP was also proven to have a role in hedgehog signaling[60-62]. In 2009, an analysis of a functional network model in Drosophila melanogaster succeeded in identifying a new role of SPOP in tumor formation and progression[63]. SPOP was also found to reduce the cellular concentration of the steroid receptor, the coactivator-3 (SRC-3) protein, suggesting SPOP as a tumor suppressor in breast cancer [64]. Other reports confirmed that SPOP mutations are a molecular subtype of prostate cancer, where SPOP is the most common mutated gene in localized prostate cancer, seen mutated in many of the studied cases[65]. SPOP acts and functions as a double-edged sword, either a tumor suppressor or tumor promoter, based on its status. A mutated SPOP gene or changes in the protein expression level, are in one way or another connected to cancer formation or progression in many cancers[66].

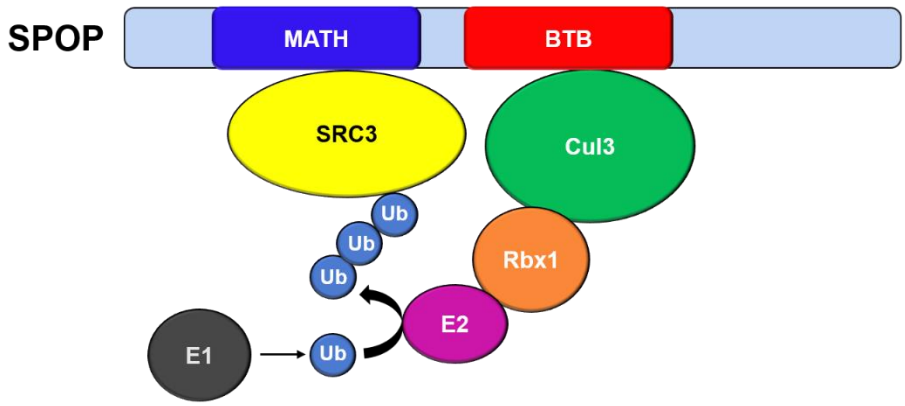

Figure 1.4 SPOP as a substrate adapter for CUL3-based ubiquitin ligases (CRL3): the SPOP-BTB domain assembles with CUL3, building the ubiquitin ligase complex and making a two-substrate binding site that will lead to ubiquitination and protein degradation. Mutations in the MATH domain prevent SPOP binding with SRC-3 protein and cannot promote its degradation.

1.4.3 SPOP Domains

SPOP is a substrate adapter for CUL3-based ubiquitin ligases (CRL3). It has 374 amino acids and consists of three structural domains. Proteins with more than one interaction domain may allow multiprotein complexes to form. The MATH (meprin and TRAF-homology) N-terminal domain recruits proteins and kinases by binding, which affects their ability to control cell survival, proliferation, and death signaling[67]. Interestingly, to date, all SPOP mutations in prostate cancer are in the MATH domain[65]. The BTB (Broad-complex, Tramtrack, Bric-a-brac)/POZ domain was found to be the domain that helps with SPOP dimerization, and it contains the binding site to the E3 ubiquitin ligase cullin-3, forming the complex which serves for protein ubiquitination. Finally, the SPOP C-terminal domain that includes the second part for dimerization facilitates the formation of large oligomers. There are 150 proteins with known and recognizable BTB domains[68]. Figure 1.4 shows how the dimeric SPOP-BTB domain assembles with CUL3, building the ubiquitin ligase and creating a two-substrate binding site. This unique structure mediates ubiquitination and protein

degradation[69]. The CRL3 complex is comprised of the CUL3 and RING protein RBX1, making a complex with the BTB-SPOP domain (SPOP/Cul3/Rbx1) which functions as an adaptor for substrate binding[59, 64].

1.4.4 SPOP in Cancer

Although most of the research in SPOP addresses its involvement in prostate cancer, several reports have shown SPOP participating in other cancer subtypes. Some of these reports suggest changes of SPOP expression in ovarian cancer[70], liver cancer (where a mutation in serine119 was found to be similar to one of the SPOP mutations in prostate cancer[71]), and in breast cancer (here, a change in SPOP genomic DNA[64] or SPOP affects the progesterone expression level through degradation[72]). Additionally, SPOP expression is lost in lung[73], gastric[74, 75], and colorectal[74, 76] cancers, and in brain tumors[77, 78]. Looking at these reports and many others shows how powerful SPOP is as a tumor suppressor, and any changes caused by mutation or protein expression lead to tumor progression.

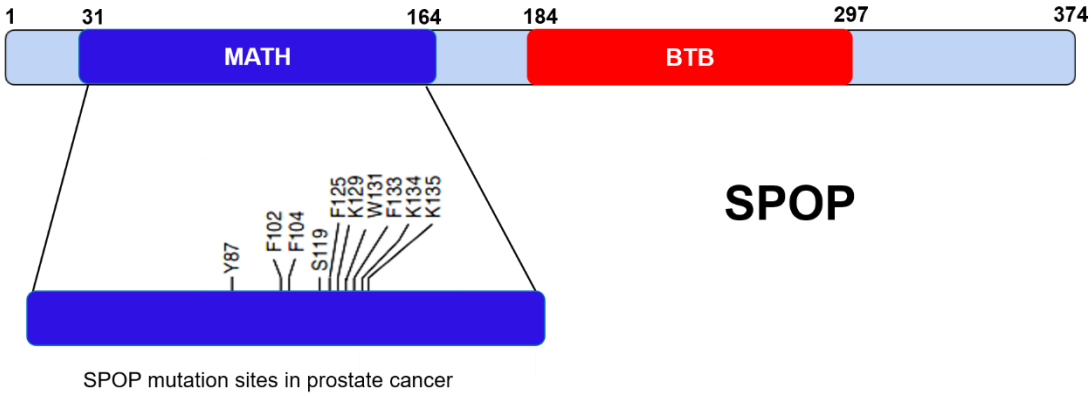

Figure 1.5 Schematic overview of the SPOP gene and sites of mutation in prostate cancer. All SPOP mutation sites in prostate cancer are clustering in the MATH domain. Mutant SPOP cannot bind to its substrates or cause their degradation.

1.4.5 SPOP in Prostate Cancer

SPOP is mutated in prostate cancer[7, 65] and endometrial cancer[79]. However, each has different mutation sites[79]. Many reports suggest that SPOP mutation might occur in the early stages of the disease[80 81]. Almost all of them report that SPOP mutations in cancer are found in the MATH domain of SPOP[79]. Figure 1.5 shows the SPOP mutated sites clustering in the MATH domain in prostate cancer [79]. Figure 1.6 illustrates the binding mechanism of wild-type SPOP to its substrate. It also illustrates the inability of the substrate to bind to mutated SPOP, and shows how the mutated substrate does not bind to wild-type SPOP[79]

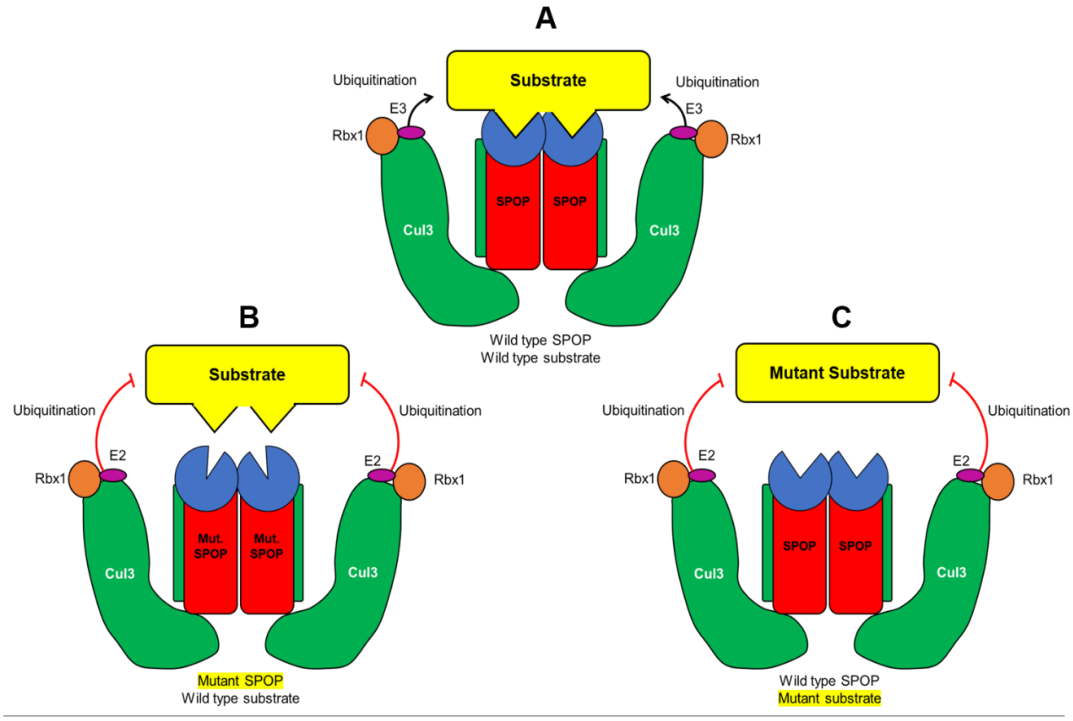

Adapted from Mani RS. 2014 *Elsevier Ltd.*

Figure 1.6 The proposed mechanism of SPOP binding to its substrate. (A) Illustrates the substrate binding to wild-SPOP, inducing protein ubiquitination. (B) The inability of the substrate to bind to mutated SPOP. (C) The mutated substrate is not binding to wild-type SPOP, (SPOP domains are shown in blue: MATH domain, Red: BTB domain, and green: BACK domain).

1.5 Y-box binding protein (YBX1)

Y-box binding protein (YBX1) is also called YB1. It belongs to the DNA/RNA-binding family, which has a highly conserved cold-shock domain (CSD) and has several interacting partners[82, 83]. YBX1 participates in a variety of cellular processes in eukaryotic cells[82-85]. Figure 1.7 is a schematic diagram adopted from C. Kosnopfel et al. / *Cell Biology*, showing the YBX-1 protein structure, domains, and functions, with possible therapeutic methods.

1.5.1 YBX1 structure and function

The human YBX1 is coded by a gene known to be in chromosome 1 (1p34) and has eight exons and seven introns that span a 19.2kb genomic region. A comprehensive review of YBX structures and function by Eliseeva et al, 2011, mentions the promoter of YBX1 as being similar to the housekeeping gene structure that consists of the E-boxes and the GC-repeats, which is very important for YBX1 transcription into 1.5kb long mRNA, and is involved in the regulation of cell division, differentiation, apoptosis, stress, and immune respons[86-88].

YBX1 consists of 324 amino acids, which translates to a size of ~36 kDa. However, in SDS-PAGE protein gels, it appears at around 48-50 kDa[89], presumably due to other posttranslational modifications. YBX1 protein is one of three subfamilies of Y-box binding proteins, where each has three domains possessing specific activities[83, 90]. Figure 1.7 is a schematic diagram representing the YBX1 domains and functions: A rich Alanine and Proline A/P N-terminal domain, a highly conserved CSD domain (which behaves as a nucleic acid binding domain that

interacts with DNA and RNA), and the C-terminal domain (CTD), which contains alternating positively- and negatively- charged amino-acid clusters, making it a hydrophilic domain that is known to bind to nucleic acids and other proteins[83, 86, 91]. Moreover, it was reported that this CTD region of YBX1 can also bind YBX1[83]. The importance of the CTD region was highlighted since the amino-acid 186-205, a non-canonical nuclear localization signal (NLS), was discovered controlling the distribution of YBX1 in the nucleus, while the amino acid 267-293 is the cytoplasmic retention site (CRS) which leads YBX1 to the cytoplasm[83, 86]. YBX1 was difficult to study using several methods, including NMR and X-ray due to its instability. To date, the only available solved structure of YBX-1 is the CSD domain[87, 91].

YBX1 protein, which is present in all type of cells, is associated with cell growth and has diverse biological functions, both in the nucleus and the cytoplasm[92]. It participates in a variety of cellular pathways and is involved in the regulation of pre-mRNA alternative splicing, stabilizing mRNA in the cytoplasm. It also engages in translation by mediating the interaction between the mRNA and the cell's initiation factors[93], and its inactivation causes embryonic lethality[94].

1.5.2 YBX1 in cancer

Considering how vital YBX1 is in normal cells where it is ubiquitously expressed, it is not surprising that YBX1 is highly over-expressed in multiple cancer types, and that it regulates tumor cell proliferation, apoptosis, invasion, and migration, including chemoresistance [95]. Several studies show increased YBX1 protein expression in cancers such as melanoma[96] osteosarcoma, squamous cell[88], lung[97],

ovarian, thyroid, colorectal (CRC)[88], colon[98] and pancreatic cancer[99]. In a study of Chordoma, a rare type of bone cancer that typically occurs along the spine, anywhere from the tailbone to the base of the skull, it was found that YBX1 promoted tumorigenesis and progression of cancer through the EGFR/AKT pathway[84]. YBX1 upregulation also occurs during breast cancer, where tRNA-derived fragments (tRFs) bind YBX1 and displace several oncogenic transcripts from YBX1, suppressing YBX1 activity[100].

1.5.3 YBX1 in prostate cancer

YBX1 has been implicated in prostate cancer as well. In a mouse xenograft model study, YBX1 was found to be up-regulated during the disease progression and androgen receptor ablation, concluding that YBX1 might cause the transformation of Prostate cancer into CRPC and further suggesting that the interaction between androgen and androgen receptor signaling causes the pathogenicity of prostate cancer[101].

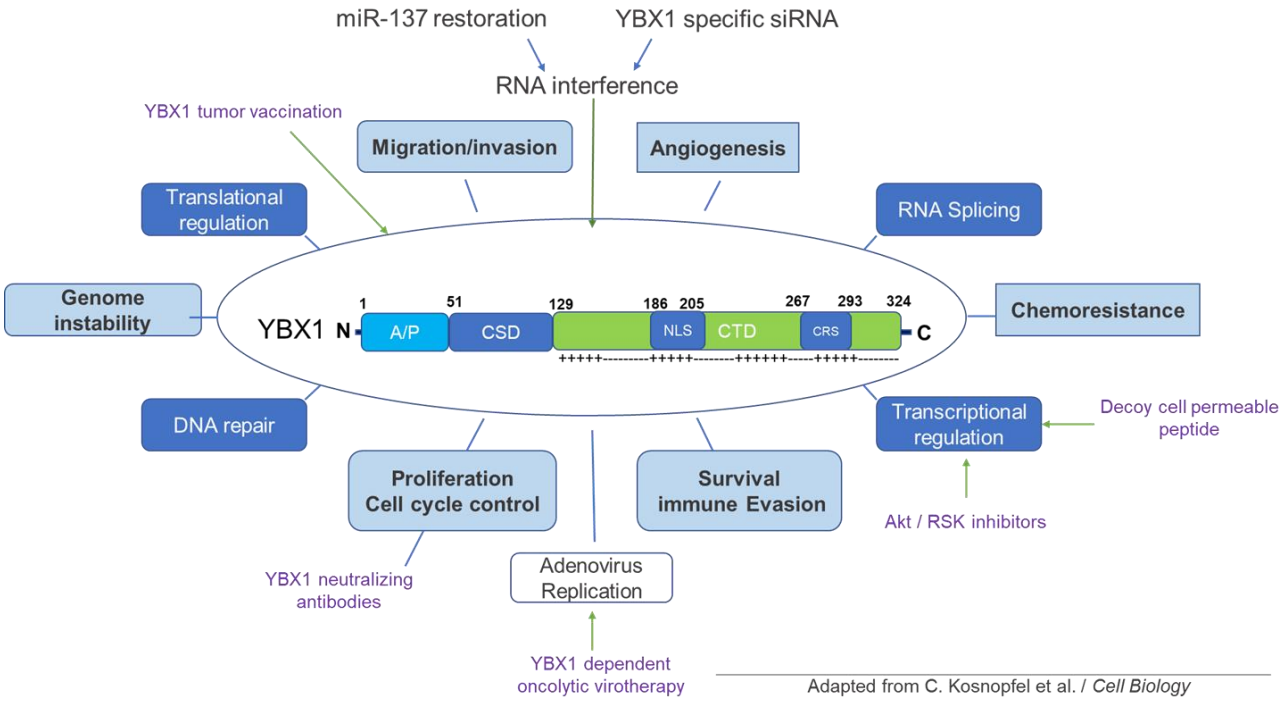

Figure 1.7 Schematic diagram of YBX-1 protein structure, functions and possible therapeutic strategies. The C-terminal domain of YB-1 consists of four alternating clusters of basic and acidic amino acids. YBX-1 is acting both as a transcription and translation factor. Along with being involved directly in pre-mRNA splicing, mRNA translation and DNA replication and repair, YBX-1 can affect many pro-tumorigenic events (light-blue boxes) participating in cancer progression. Possible therapeutic strategies are presented (purple color)

1.5.4 References

1. Mollica, V.; Di Nunno, V.; Cimadamore, A.; Lopez-Beltran, A.; Cheng, L.; Santoni, M.; Scarpelli, M.; Montironi, R.; Massari, F., Molecular Mechanisms Related to Hormone Inhibition Resistance in Prostate Cancer. *Cells* **2019,** *8* (1).

2. Willems, E.; Dedobbeleer, M.; Digregorio, M.; Lombard, A.; Lumapat, P. N.; Rogister, B., The functional diversity of Aurora kinases: a comprehensive review. *Cell Div* **2018,** *13*, 7.

3. MPH, R. L. S. M. K. D. M.; Ahmedin Jemal DVM, P., Cancer statistics, 2019. *CA: A Cancer Journal for clinicians* **2019,** *69* (1).

4. Cooperberg, M. R., Re: Follow-up of Prostatectomy Versus Observation for Early Prostate Cancer. *Eur Urol* **2017**.

5. Coutinho, I.; Day, T. K.; Tilley, W. D.; Selth, L. A., Androgen receptor signaling in castration-resistant prostate cancer: a lesson in persistence. *Endocr Relat Cancer* **2016,** *23* (12), T179-T197.

6. Russo, A.; Manna, S. L.; Novellino, E.; Malfitano, A. M.; Marasco, D., Molecular signaling involving intrinsically disordered proteins in prostate cancer. *Asian J Androl* **2016,** *18* (5), 673-81.

7. Brenner, J. C.; Chinnaiyan, A. M., Disruptive events in the life of prostate cancer. *Cancer Cell* **2011,** *19* (3), 301-3.

8. Ciccarese, C.; Massari, F.; Iacovelli, R.; Fiorentino, M.; Montironi, R.; Di Nunno, V.; Giunchi, F.; Brunelli, M.; Tortora, G., Prostate cancer heterogeneity: Discovering novel molecular targets for therapy. *Cancer Treat Rev* **2017,** *54*, 68-73.

9. Scott, R. W.; Olson, M. F., LIM kinases: function, regulation and association with human disease. *J Mol Med (Berl)* **2007,** *85* (6), 555-68.

10. Bach, I., The LIM domain: regulation by association. *Mech Dev* **2000,** *91* (1-2), 5-17.

11. Bernard, O.; Ganiatsas, S.; Kannourakis, G.; Dringen, R., Kiz-1, a protein with LIM zinc finger and kinase domains, is expressed mainly in neurons. *Cell Growth Differ* **1994,** *5* (11), 1159-71.

12. Nagata, K.; Ohashi, K.; Yang, N.; Mizuno, K., The N-terminal LIM domain negatively regulates the kinase activity of LIM-kinase 1. *Biochem J* **1999,** *343 Pt 1*, 99-105.

13. Tomiyoshi, G.; Horita, Y.; Nishita, M.; Ohashi, K.; Mizuno, K., Caspase-mediated cleavage and activation of LIM-kinase 1 and its role in apoptotic membrane blebbing. *Genes Cells* **2004,** *9* (6), 591-600.

14. Nishiya, N.; Sabe, H.; Nose, K.; Shibanuma, M., The LIM domains of hic-5 protein recognize specific DNA fragments in a zinc-dependent manner in vitro. *Nucleic Acids Res* **1998,** *26* (18), 4267-73.

15. Yang, N.; Mizuno, K., Nuclear export of LIM-kinase 1, mediated by two leucine-rich nuclear-export signals within the PDZ domain. *The Biochemical journal* **1999,** *338 (Pt 3)*, 793.

16. Yang, N.; Higuchi, O.; Mizuno, K., Cytoplasmic Localization of LIM-Kinase 1 Is Directed by a Short Sequence within the PDZ Domain. *Experimental Cell Research* **1998,** *241* (1), 242-252.

17. Goyal, P.; Pandey, D.; Siess, W., Phosphorylation-dependent regulation of unique nuclear and nucleolar localization signals of LIM kinase 2 in endothelial cells. *J Biol Chem* **2006,** *281* (35), 25223-30.

18. Amano, T.; Tanabe, K.; Eto, T.; Narumiya, S.; Mizuno, K., LIM-kinase 2 induces formation of stress fibres, focal adhesions and membrane blebs, dependent on its activation by Rho-associated kinase-catalysed phosphorylation at threonine-505. *Biochem. J.* **2001,** *354*, 149-159.

19. Sumi, T.; Matsumoto, K.; Shibuya, A.; Nakamura, T., Activation of LIM kinases by myotonic dystrophy kinase-related Cdc42-binding kinase alpha. *The Journal of biological chemistry* **2001,** *276* (25), 23092.

20. Goyal, P.; Pandey, D.; Behring, A.; Siess, W., Inhibition of nuclear import of LIMK2 in endothelial cells by protein kinase C-dependent phosphorylation at Ser-283. *J Biol Chem* **2005,** *280* (30), 27569-77.

21. Johnson, E. O.; Chang, K. H.; Ghosh, S.; Venkatesh, C.; Giger, K.; Low, P. S.; Shah, K., LIMK2 is a crucial regulator and effector of Aurora-A-kinase-mediated malignancy. *J Cell Sci* **2012,** *125* (Pt 5), 1204-16.

22. Vardouli, L.; Moustakas, A.; Stournaras, C., LIM-kinase 2 and cofilin phosphorylation mediate actin cytoskeleton reorganization induced by transforming growth factor-beta. *J Biol Chem* **2005,** *280* (12), 11448-57.

23. Lagoutte, E.; Villeneuve, C.; Lafanechère, L.; Wells, C. M.; Jones, G. E.; Chavrier, P.; Rossé, C., LIMK Regulates Tumor-Cell Invasion and Matrix Degradation Through Tyrosine Phosphorylation of MT1-MMP. *Sci Rep* **2016,** *6*, 24925.

24. Shea, K. F.; Wells, C. M.; Garner, A. P.; Jones, G. E., ROCK1 and LIMK2 interact in spread but not blebbing cancer cells. *PLoS One* **2008,** *3* (10), e3398.

25. Vlecken, D. H.; Bagowski, C. P., LIMK1 and LIMK2 are important for metastatic behavior and tumor cell-induced angiogenesis of pancreatic cancer cells. *Zebrafish* **2009,** *6* (4), 433-9.

26. Johnson, E. O.; Chang, K.-H.; Ghosh, S.; Venkatesh, C.; Giger, K.; Low, P. S.; Shah, K., LIMK2 is a crucial regulator and effector of Aurora-A-kinase-mediated malignancy. *Journal of cell science* **2012,** *125* (Pt 5), 1204.

27. Aggelou, H.; Chadla, P.; Nikou, S.; Karteri, S.; Maroulis, I.; Kalofonos, H. P.; Papadaki, H.; Bravou, V., LIMK/cofilin pathway and Slingshot are implicated in human colorectal cancer progression and chemoresistance. *Virchows Arch* **2018,** *472* (5), 727-737.

28. Nikhil, K.; Chang, L.; Viccaro, K.; Jacobsen, M.; McGuire, C.; Satapathy, S. R.; Tandiary, M.; Broman, M. M.; Cresswell, G.; He, Y. J.; Sandusky, G. E.; Ratliff, T. L.; Chowdhury, D.; Shah, K., Identification of LIMK2 as a Therapeutic Target in Castration Resistant Prostate Cancer. *Cancer Lett* **2019**.

29. Levinson, N. M., The multifaceted allosteric regulation of Aurora kinase A. *Biochem J* **2018,** *475* (12), 2025-2042.

30. Yan, M.; Wang, C.; He, B.; Yang, M.; Tong, M.; Long, Z.; Liu, B.; Peng, F.; Xu, L.; Zhang, Y.; Liang, D.; Lei, H.; Subrata, S.; Kelley, K. W.; Lam, E. W.; Jin, B.; Liu, Q., Aurora-A Kinase: A Potent Oncogene and Target for Cancer Therapy. *Med Res Rev* **2016,** *36* (6), 1036-1079.

31. Kinoshita, K.; Noetzel, T. L.; Pelletier, L.; Mechtler, K.; Drechsel, D. N.; Schwager, A.; Lee, M.; Raff, J. W.; Hyman, A. A., Aurora A phosphorylation of TACC3/maskin is required for centrosome-dependent microtubule assembly in mitosis.(Author Abstract). *The Journal of Cell Biology* **2005,** *170* (7), 1047.

32. Bellanger, J. M.; Gönczy, P., TAC-1 and ZYG-9 form a complex that promotes microtubule assembly in C. elegans embryos. *Curr Biol* **2003,** *13* (17), 1488-98.

33. Tang, A.; Gao, K.; Chu, L.; Zhang, R.; Yang, J.; Zheng, J., Aurora kinases: novel therapy targets in cancers. *Oncotarget* **2017,** *8* (14), 23937-23954.

34. Yang, N.; Wang, C.; Wang, Z.; Zona, S.; Lin, S. X.; Wang, X.; Yan, M.; Zheng, F. M.; Li, S. S.; Xu, B.; Bella, L.; Yong, J. S.; Lam, E. W.; Liu, Q., FOXM1 recruits nuclear Aurora kinase A to participate in a positive feedback loop essential for the self-renewal of breast cancer stem cells. *Oncogene* **2017,** *36* (24), 3428-3440.

35. Cirak, Y.; Furuncuoglu, Y.; Yapicier, O.; Aksu, A.; Cubukcu, E., Aurora A overexpression in breast cancer patients induces taxane resistance and results in worse prognosis. *J BUON* **2015,** *20* (6), 1414-9.

36. Do, T. V.; Xiao, F.; Bickel, L. E.; Klein-Szanto, A. J.; Pathak, H. B.; Hua, X.; Howe, C.; O'Brien, S. W.; Maglaty, M.; Ecsedy, J. A.; Litwin, S.; Golemis, E. A.; Schilder, R. J.; Godwin, A. K.; Connolly, D. C., Aurora kinase A mediates epithelial ovarian cancer cell migration and adhesion. *Oncogene* **2014,** *33* (5), 539-49.

37. Liu, W.; Lu, Y.; Chai, X.; Liu, X.; Zhu, T.; Wu, X.; Fang, Y.; Zhang, X., Antitumor activity of TY-011 against gastric cancer by inhibiting Aurora A, Aurora B and VEGFR2 kinases. *J Exp Clin Cancer Res* **2016,** *35* (1), 183.

38. Casorzo, L.; Dell'Aglio, C.; Sarotto, I.; Risio, M., Aurora kinase A gene copy number is associated with the malignant transformation of colorectal adenomas but not with the serrated neoplasia progression. *Hum Pathol* **2015,** *46* (3), 411-8.

39. Chuang, T. P.; Wang, J. Y.; Jao, S. W.; Wu, C. C.; Chen, J. H.; Hsiao, K. H.; Lin, C. Y.; Chen, S. H.; Su, S. Y.; Chen, Y. J.; Chen, Y. T.; Wu, D. C.; Li, L. H., Over-expression of AURKA, SKA3 and DSN1 contributes to colorectal adenoma to carcinoma progression. *Oncotarget* **2016,** *7* (29), 45803-45818.

40. Wang, X.; Lu, N.; Niu, B.; Chen, X.; Xie, J.; Cheng, N., Overexpression of Aurora-A enhances invasion and matrix metalloproteinase-2 expression in esophageal squamous cell carcinoma cells. *Mol Cancer Res* **2012,** *10* (5), 588-96.

41. Lo Iacono, M.; Monica, V.; Saviozzi, S.; Ceppi, P.; Bracco, E.; Papotti, M.; Scagliotti, G. V., Aurora Kinase A expression is associated with lung cancer histological-subtypes and with tumor de-differentiation. *J Transl Med* **2011,** *9*, 100.

42. Twu, N. F.; Yuan, C. C.; Yen, M. S.; Lai, C. R.; Chao, K. C.; Wang, P. H.; Wu, H. H.; Chen, Y. J., Expression of Aurora kinase A and B in normal and malignant cervical tissue: high Aurora A kinase expression in squamous cervical cancer. *Eur J Obstet Gynecol Reprod Biol* **2009,** *142* (1), 57-63.

43. Kivinummi, K.; Urbanucci, A.; Leinonen, K.; Tammela, T. L. J.; Annala, M.; Isaacs, W. B.; Bova, G. S.; Nykter, M.; Visakorpi, T., The expression of AURKA is androgen regulated in castration-resistant prostate cancer. *Sci Rep* **2017,** *7* (1), 17978.

44. Toughiri, R.; Li, X.; Du, Q.; Bieberich, C. J., Phosphorylation of NuMA by Aurora-A kinase in PC-3 prostate cancer cells affects proliferation, survival, and interphase NuMA localization. *J Cell Biochem* **2013,** *114* (4), 823-30.

45. Premkumar, D. R.; Jane, E. P.; Pollack, I. F., Cucurbitacin-I inhibits Aurora kinase A, Aurora kinase B and survivin, induces defects in cell cycle progression and promotes ABT-737-induced cell death in a caspase-independent manner in malignant human glioma cells. *Cancer Biol Ther* **2015,** *16* (2), 233-43.

46. Kim, S. J.; Jang, J. E.; Cheong, J. W.; Eom, J. I.; Jeung, H. K.; Kim, Y.; Hwang, D. Y.; Min, Y. H., Aurora A kinase expression is increased in leukemia stem cells,

and a selective Aurora A kinase inhibitor enhances Ara-C-induced apoptosis in acute myeloid leukemia stem cells. *Korean J Hematol* **2012,** *47* (3), 178-85.

47. Tatsuka, M.; Sato, S.; Kitajima, S.; Suto, S.; Kawai, H.; Miyauchi, M.; Ogawa, I.; Maeda, M.; Ota, T.; Takata, T., Overexpression of Aurora-A potentiates HRAS-mediated oncogenic transformation and is implicated in oral carcinogenesis. *Oncogene* **2005,** *24* (6), 1122-7.

48. Li, W.; Wang, P.; Zhang, B.; Zhang, J.; Ming, J.; Xie, W.; Na, J., Differential regulation of H3S10 phosphorylation, mitosis progression and cell fate by Aurora Kinase B and C in mouse preimplantation embryos. *Protein Cell* **2017,** *8* (9), 662-674.

49. Ylipää, A.; Kivinummi, K.; Kohvakka, A.; Annala, M.; Latonen, L.; Scaravilli, M.; Kartasalo, K.; Leppänen, S. P.; Karakurt, S.; Seppälä, J.; Yli-Harja, O.; Tammela, T. L.; Zhang, W.; Visakorpi, T.; Nykter, M., Transcriptome Sequencing Reveals PCAT5 as a Novel ERG-Regulated Long Noncoding RNA in Prostate Cancer. *Cancer Res* **2015,** *75* (19), 4026-31.

50. Waltering, K. K.; Helenius, M. A.; Sahu, B.; Manni, V.; Linja, M. J.; Jänne, O. A.; Visakorpi, T., Increased expression of androgen receptor sensitizes prostate cancer cells to low levels of androgens. *Cancer Res* **2009,** *69* (20), 8141-9.

51. Urbanucci, A.; Sahu, B.; Seppälä, J.; Larjo, A.; Latonen, L. M.; Waltering, K. K.; Tammela, T. L.; Vessella, R. L.; Lähdesmäki, H.; Jänne, O. A.; Visakorpi, T., Overexpression of androgen receptor enhances the binding of the receptor to the chromatin in prostate cancer. *Oncogene* **2012,** *31* (17), 2153-63.

52. Atala, A., Re: overexpression of androgen receptor enhances the binding of the receptor to the chromatin in prostate cancer. *J Urol* **2013,** *189* (2), 769-70.

53. Beltran, H.; Oromendia, C.; Danila, D. C.; Montgomery, B.; Hoimes, C.; Szmulewitz, R. Z.; Vaishampayan, U.; Armstrong, A. J.; Stein, M.; Pinski, J.; Mosquera, J. M.; Sailer, V.; Bareja, R.; Romanel, A.; Gumpeni, N.; Sboner, A.; Dardenne, E.; Puca, L.; Prandi, D.; Rubin, M. A.; Scher, H. I.; Rickman, D. S.; Demichelis, F.; Nanus, D. M.; Ballman, K. V.; Tagawa, S. T., A Phase II Trial of the Aurora Kinase A Inhibitor Alisertib for Patients with Castration-resistant and Neuroendocrine Prostate Cancer: Efficacy and Biomarkers. *Clin Cancer Res* **2019,** *25* (1), 43-51.

54. Nagai, Y.; Kojima, T.; Muro, Y.; Hachiya, T.; Nishizawa, Y.; Wakabayashi, T.; Hagiwara, M., Identification of a novel nuclear speckle-type protein, SPOP. *FEBS Lett* **1997,** *418* (1-2), 23-6.

55. Lamond, A. I.; Spector, D. L., Nuclear speckles: a model for nuclear organelles. *Nat Rev Mol Cell Biol* **2003,** *4* (8), 605-12.

56. Handwerger, K. E.; Gall, J. G., Subnuclear organelles: new insights into form and function. *Trends Cell Biol* **2006,** *16* (1), 19-26.

57. UniProtKB, O43791 (SPOP_HUMAN). UniProt: 2019.

58. Wang, S.; Cho, Y. K., Nuclear Translocation and Degradation of Target

Proteins Using Engineered Intracellular Antibodies. In *Mira SMAR Conferencing*, 2015.

59. Kwon, J. E.; La, M.; Oh, K. H.; Oh, Y. M.; Kim, G. R.; Seol, J. H.; Baek, S. H.; Chiba, T.; Tanaka, K.; Bang, O. S.; Joe, C. O.; Chung, C. H., BTB domain-containing speckle-type POZ protein (SPOP) serves as an adaptor of Daxx for ubiquitination by Cul3-based ubiquitin ligase. *J Biol Chem* **2006,** *281* (18), 12664-72.

60. Zhang, Q.; Zhang, L.; Wang, B.; Ou, C. Y.; Chien, C. T.; Jiang, J., A hedgehog-induced BTB protein modulates hedgehog signaling by degrading Ci/Gli transcription factor. *Dev Cell* **2006,** *10* (6), 719-29.

61. Chen, M. H.; Wilson, C. W.; Li, Y. J.; Law, K. K.; Lu, C. S.; Gacayan, R.; Zhang, X.; Hui, C. C.; Chuang, P. T., Cilium-independent regulation of Gli protein function by Sufu in Hedgehog signaling is evolutionarily conserved. *Genes Dev* **2009,** *23* (16), 1910-28.

62. Wen, X.; Lai, C. K.; Evangelista, M.; Hongo, J. A.; de Sauvage, F. J.; Scales, S. J., Kinetics of hedgehog-dependent full-length Gli3 accumulation in primary cilia and subsequent degradation. *Mol Cell Biol* **2010,** *30* (8), 1910-22.

63. Liu, J.; Ghanim, M.; Xue, L.; Brown, C. D.; Iossifov, I.; Angeletti, C.; Hua, S.; Nègre, N.; Ludwig, M.; Stricker, T.; Al-Ahmadie, H. A.; Tretiakova, M.; Camp, R. L.; Perera-Alberto, M.; Rimm, D. L.; Xu, T.; Rzhetsky, A.; White, K. P., Analysis of Drosophila segmentation network identifies a JNK pathway factor overexpressed in kidney cancer. *Science* **2009,** *323* (5918), 1218-22.

64. Li, C.; Ao, J.; Fu, J.; Lee, D. F.; Xu, J.; Lonard, D.; O'Malley, B. W., Tumor-suppressor role for the SPOP ubiquitin ligase in signal-dependent proteolysis of the oncogenic co-activator SRC-3/AIB1. *Oncogene* **2011,** *30* (42), 4350-64.

65. Barbieri, C. E.; Baca, S. C.; Lawrence, M. S.; Demichelis, F.; Blattner, M.; Theurillat, J. P.; White, T. A.; Stojanov, P.; Van Allen, E.; Stransky, N.; Nickerson, E.; Chae, S. S.; Boysen, G.; Auclair, D.; Onofrio, R. C.; Park, K.; Kitabayashi, N.; MacDonald, T. Y.; Sheikh, K.; Vuong, T.; Guiducci, C.; Cibulskis, K.; Sivachenko, A.; Carter, S. L.; Saksena, G.; Voet, D.; Hussain, W. M.; Ramos, A. H.; Winckler, W.; Redman, M. C.; Ardlie, K.; Tewari, A. K.; Mosquera, J. M.; Rupp, N.; Wild, P. J.; Moch, H.; Morrissey, C.; Nelson, P. S.; Kantoff, P. W.; Gabriel, S. B.; Golub, T. R.; Meyerson, M.; Lander, E. S.; Getz, G.; Rubin, M. A.; Garraway, L. A., Exome sequencing identifies recurrent SPOP, FOXA1 and MED12 mutations in prostate cancer. *Nat Genet* **2012,** *44* (6), 685-9.

66. Cheng, J.; Guo, J.; Wang, Z.; North, B. J.; Tao, K.; Dai, X.; Wei, W., Functional analysis of Cullin 3 E3 ligases in tumorigenesis. *Biochim Biophys Acta Rev Cancer* **2018,** *1869* (1), 11-28.

67. Takahashi, I.; Kameoka, Y.; Hashimoto, K., MacroH2A1.2 binds the nuclear protein Spop. *Biochim Biophys Acta* **2002,** *1591* (1-3), 63-8.

68. Zhuang, M.; Calabrese, M. F.; Liu, J.; Waddell, M. B.; Nourse, A.; Hammel, M.; Miller, D. J.; Walden, H.; Duda, D. M.; Seyedin, S. N.; Hoggard, T.; Harper, J. W.; White, K. P.; Schulman, B. A., Structures of SPOP-substrate complexes: insights into molecular architectures of BTB-Cul3 ubiquitin ligases. *Mol Cell* **2009,** *36* (1), 39-50.

69. Choo, K. B.; Chuang, T. J.; Lin, W. Y.; Chang, C. M.; Tsai, Y. H.; Huang, C. J., Evolutionary expansion of SPOP and associated TD/POZ gene family: impact of evolutionary route on gene expression pattern. *Gene* **2010,** *460* (1-2), 39-47.

70. Arildsen, N. S.; Jönsson, J. M.; Bartuma, K.; Ebbesson, A.; Westbom-Fremer, S.; Måsbäck, A.; Malander, S.; Nilbert, M.; Hedenfalk, I. A., Involvement of Chromatin Remodeling Genes and the Rho GTPases. *Front Oncol* **2017,** *7*, 109.

71. Jia, D.; Dong, R.; Jing, Y.; Xu, D.; Wang, Q.; Chen, L.; Li, Q.; Huang, Y.; Zhang, Y.; Zhang, Z.; Liu, L.; Zheng, S.; Xia, Q.; Wang, H.; Dong, K.; He, X., Exome sequencing of hepatoblastoma reveals novel mutations and cancer genes in the Wnt pathway and ubiquitin ligase complex. *Hepatology* **2014,** *60* (5), 1686-96.

72. Gao, K.; Jin, X.; Tang, Y.; Ma, J.; Peng, J.; Yu, L.; Zhang, P.; Wang, C., Tumor suppressor SPOP mediates the proteasomal degradation of progesterone receptors (PRs) in breast cancer cells. *Am J Cancer Res* **2015,** *5* (10), 3210-20.

73. Li, J.-J.; Zhang, J.-F.; Yao, S.-M.; Huang, H.; Zhang, S.; Zhao, M.; Huang, J.-A., Decreased expression of speckle-type POZ protein for the prediction of poor prognosis in patients with non-small cell lung cancer. *Oncology Letters* **2017,** *14* (3), 2743.

74. Kim, M. S.; Je, E. M.; Oh, J. E.; Yoo, N. J.; Lee, S. H., Mutational and expressional analyses of SPOP, a candidate tumor suppressor gene, in prostate, gastric and colorectal cancers. *APMIS* **2013,** *121* (7), 626-33.

75. Zeng, C.; Wang, Y.; Lu, Q.; Chen, J.; Zhang, J.; Liu, T.; Lv, N.; Luo, S., SPOP suppresses tumorigenesis by regulating Hedgehog/Gli2 signaling pathway in gastric cancer. *Journal of experimental & clinical cancer research : CR* **2014,** *33* (1), 75.

76. Xiaofei, Z.; Jinqiu, T.; Lei, Z.; Ran, T.; Lilin, M.; Jun, Q., Silencing speckle-type POZ protein by promoter hypermethylation decreases cell apoptosis through upregulating Hedgehog signaling pathway in colorectal cancer. *Cell Death and Disease* **2016,** *7* (12), e2569.

77. Hu, Y.; Yang, L.; Zhang, M.; Huang, Z.; Lin, J.; Zhang, N., Expression and clinical relevance of SPOPL in medulloblastoma. *Oncology Letters* **2017,** *14* (3), 3051.

78. Ding, D.; Song, T.; Jun, W.; Tan, Z.; Fang, J., Decreased expression of the SPOP gene is associated with poor prognosis in glioma.(speckle-type POZ protein)(Report). *International Journal of Oncology* **2015,** *46* (1), 333.

79. Mani, R. S., The emerging role of speckle-type POZ protein (SPOP) in cancer development. *Drug Discov Today* **2014,** *19* (9), 1498-502.

80. Blattner, M.; Lee, D. J.; O'Reilly, C.; Park, K.; MacDonald, T. Y.; Khani, F.; Turner, K. R.; Chiu, Y. L.; Wild, P. J.; Dolgalev, I.; Heguy, A.; Sboner, A.; Ramazangolu, S.; Hieronymus, H.; Sawyers, C.; Tewari, A. K.; Moch, H.; Yoon, G. S.; Known, Y. C.; Andrén, O.; Fall, K.; Demichelis, F.; Mosquera, J. M.; Robinson, B. D.; Barbieri, C. E.; Rubin, M. A., SPOP mutations in prostate cancer across demographically diverse patient cohorts. *Neoplasia* **2014,** *16* (1), 14-20.

81. Blattner, M.; Liu, D.; Robinson, B. D.; Huang, D.; Poliakov, A.; Gao, D.; Nataraj, S.; Deonarine, L. D.; Augello, M. A.; Sailer, V.; Ponnala, L.; Ittmann, M.; Chinnaiyan, A. M.; Sboner, A.; Chen, Y.; Rubin, M. A.; Barbieri, C. E., SPOP Mutation Drives Prostate Tumorigenesis In Vivo through Coordinate Regulation of PI3K/mTOR and AR Signaling. *Cancer Cell* **2017,** *31* (3), 436-451.

82. Chao, H. M.; Huang, H. X.; Chang, P. H.; Tseng, K. C.; Miyajima, A.; Chern, E., Y-box binding protein-1 promotes hepatocellular carcinoma-initiating cell progression and tumorigenesis via Wnt/β-catenin pathway. *Oncotarget* **2017,** *8* (2), 2604-2616.

83. Kosnopfel, C.; Sinnberg, T.; Schittek, B., Y-box binding protein 1--a prognostic marker and target in tumour therapy. *Eur J Cell Biol* **2014,** *93* (1-2), 61-70.

84. Liang, C.; Ma, Y.; Yong, L.; Yang, C.; Wang, P.; Liu, X.; Zhu, B.; Zhou, H.; Liu, Z., Y-box binding protein-1 promotes tumorigenesis and progression via the epidermal growth factor receptor/AKT pathway in spinal chordoma. *Cancer Sci* **2019,** *110* (1), 166-179.

85. Wolffe, A. P.; Tafuri, S.; Ranjan, M.; Familari, M., THE Y-BOX FACTORS - A FAMILY OF NUCLEIC-ACID BINDING-PROTEINS CONSERVED FROM ESCHERICHIA-COLI TO MAN. *New Biologist* **1992,** *4* (4), 290-298.

86. Eliseeva, I. A.; Kim, E. R.; Guryanov, S. G.; Ovchinnikov, L. P.; Lyabin, D. N., Y-box-binding protein 1 (YB-1) and its functions. *Biochemistry (Mosc)* **2011,** *76* (13), 1402-33.

87. Kljashtorny, V.; Nikonov, S.; Ovchinnikov, L.; Lyabin, D.; Vodovar, N.; Curmi, P.; Manivet, P., The Cold Shock Domain of YB-1 Segregates RNA from DNA by Non-Bonded Interactions. *PLoS One* **2015,** *10* (7), e0130318.

88. Prabhu, L.; Mundade, R.; Wang, B.; Wei, H.; Hartley, A. V.; Martin, M.; McElyea, K.; Temm, C. J.; Sandusky, G.; Liu, Y.; Lu, T., Critical role of phosphorylation of serine 165 of YBX1 on the activation of NF-κB in colon cancer. *Oncotarget* **2015,** *6* (30), 29396-412.

89. Cohen, S. B.; Ma, W.; Valova, V. A.; Algie, M.; Harfoot, R.; Woolley, A. G.; Robinson, P. J.; Braithwaite, A. W., Genotoxic stress-induced nuclear localization of oncoprotein YB-1 in the absence of proteolytic processing. *Oncogene* **2009,** *29* (3), 403.

90. Wolffe, A. P., Structural and functional properties of the evolutionarily ancient Y-box family of nucleic acid binding proteins. Hoboken, 1994; Vol. 16, pp 245-251.

91. Kloks, C. P.; Spronk, C. A.; Lasonder, E.; Hoffmann, A.; Vuister, G. W.; Grzesiek, S.; Hilbers, C. W., The solution structure and DNA-binding properties of the cold-shock domain of the human Y-box protein YB-1. *J Mol Biol* **2002,** *316* (2), 317-26.

92. Kohno, K.; Izumi, H.; Uchiumi, T.; Ashizuka, M.; Kuwano, M., The pleiotropic functions of the Y-box-binding protein, YB-1. Hoboken, 2003; Vol. 25, pp 691-698.

93. Chen, C. Y.; Gherzi, R.; Andersen, J. S.; Gaietta, G.; Jürchott, K.; Royer, H. D.; Mann, M.; Karin, M., Nucleolin and YB-1 are required for JNK-mediated interleukin-2 mRNA stabilization during T-cell activation. *Genes Dev* **2000,** *14* (10), 1236-48.

94. Uchiumi, T.; Fotovati, A.; Sasaguri, T.; Shibahara, K.; Shimada, T.; Fukuda, T.; Nakamura, T.; Izumi, H.; Tsuzuki, T.; Kuwano, M.; Kohno, K., YB-1 is important for an early stage embryonic development: neural tube formation and cell proliferation. *J Biol Chem* **2006,** *281* (52), 40440-9.

95. El-Naggar, Amal m.; Veinotte, Chansey j.; Cheng, H.; Grunewald, Thomas g. P.; Negri, Gian l.; Somasekharan, Syam p.; Corkery, Dale p.; Tirode, F.; Mathers, J.; Khan, D.; Kyle, Alastair h.; Baker, Jennifer h.; Lepard, Nancy e.; McKinney, S.; Hajee, S.; Bosiljcic, M.; Leprivier, G.; Tognon, Cristina e.; Minchinton, Andrew i.; Bennewith, Kevin l.; Delattre, O.; Wang, Y.; Dellaire, G.; Berman, Jason n.; Sorensen, Poul h., Translational Activation of HIF1α by YB-1 Promotes Sarcoma Metastasis. *Cancer Cell* **2015,** *27* (5), 682-697.

96. Schittek, B.; Psenner, K.; Sauer, B.; Meier, F.; Iftner, T.; Garbe, C., The increased expression of Y box-binding protein 1 in melanoma stimulates proliferation and tumor invasion, antagonizes apoptosis and enhances chemoresistance. *International Journal of Cancer* **2007,** *120* (10), 2110-2118.

97. Murugesan, S. N.; Yadav, B. S.; Maurya, P. K.; Chaudhary, A.; Singh, S.; Mani, A., Expression and network analysis of YBX1 interactors for identification of new drug targets in lung adenocarcinoma. *J Genomics* **2018,** *6*, 103-112.

98. Martin, M.; Hua, L.; Wang, B.; Wei, H.; Prabhu, L.; Hartley, A. V.; Jiang, G.; Liu, Y.; Lu, T., Novel Serine 176 Phosphorylation of YBX1 Activates NF-κB in Colon Cancer. *J Biol Chem* **2017,** *292* (8), 3433-3444.

99. Shinkai, K.; Nakano, K.; Cui, L.; Mizuuchi, Y.; Onishi, H.; Oda, Y.; Obika, S.; Tanaka, M.; Katano, M., Nuclear expression of Y-box binding protein-1 is associated with poor prognosis in patients with pancreatic cancer and its knockdown inhibits tumor growth and metastasis in mice tumor models. *International Journal of Cancer* **2016,** *139* (2), 433-445.

100. Goodarzi, H.; Liu, X.; Nguyen, Hoang c. B.; Zhang, S.; Fish, L.; Tavazoie, Sohail f., Endogenous tRNA-Derived Fragments Suppress Breast Cancer Progression via YBX1 Displacement. *Cell* **2015,** *161* (4), 790-802.

101. Giménez-Bonafé, P.; Fedoruk, M. N.; Whitmore, T. G.; Akbari, M.; Ralph, J. L.; Ettinger, S.; Gleave, M. E.; Nelson, C. C., YB-1 is upregulated during prostate cancer tumor progression and increases P-glycoprotein activity. *Prostate* **2004,** *59* (3), 337-349.

CHAPTER 2. SPOP IS A DIRECT SUBSTRATE FOR LIMK2

2.1 Introduction

LIMK2 regulates actin cytoskeletal dynamics, mediating the regulation of cell morphology and motility[1, 2]. Up until now, Cofilin, MT1-MMP (membrane type 1-matrix metalloproteinase) and TWIST1 are the only substrates that have been identified for LIMK2[3]. Direct phosphorylation of cofilin by LIMK2 mediates the regulation of actin dynamics by inhibiting its depolymerization[2, 4, 5]. The phosphorylation of MT1-MMP regulates tumor growth and cell migration in breast cancer[6]. We identified LIMK2 as an excellent target for castration-resistant prostate cancer (CRPC)[3].

Speckle-type POZ protein (SPOP) is well known to be mutated in prostate cancer[7, 8]. The MATH and BTB domains of SPOP are essential parts of the ubiquitin ligase complex. Figure 1.4 in Chapter 1 shows the direct interaction between SPOP and SRC3, where SPOP promotes its ubiquitination and proteolysis in breast cancer. This occurs via Cullin3, causing SRC3 to bind to the BTB-SPOP domain [9].

In this study, we have identified SPOP as a novel substrate for LIMK2 by direct phosphorylation using in-vitro kinase assays. Our results were supported by initial studies in C4-2 and 22Rv1 PCa cells, which showed that LIMK2 negatively regulates SPOP at the protein level. Subsequently, we identified the SPOP phosphorylation sites using site-

directed mutagenesis, a method that involved mutating the predicted sites and looking for a reduction in phosphorylation.

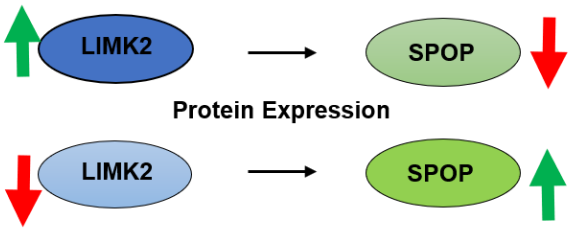

2.2 Results

2.2.1 LIMK2 regulates SPOP at the protein expression level

Previous studies from our lab have shown that the overexpression of LIMK2 affects the expression of SPOP in C4-2 and 22Rv1 prostate cancer cell lines (Figure 2.1). The results showed that LIMK2 does not regulate SPOP at the transcriptional level (data is not included), but at a translational level. While LIMK2 overexpression was found to decreased SPOP protein levels, LIMK2 knockdown showed the opposite effect, concluding an inverse relationship between LIMK2 protein expression and SPOP levels in human prostate cancer cell lines.

2.2.2 SPOP alteration of LIMK2 protein expression level

To further investigate the relationship between LIMK2 and SPOP, our lab experimented with SPOP overexpression and knockdown in both C4-2 and 22Rv1 cancer cell lines. The overexpression of SPOP protein decreased the protein level of LIMK2 in C4-2 cells, but not in 22Rv1 cells. Knocking down SPOP protein levels using shRNA increased the

LIMK2 protein level significantly in both C4-2 cells, and 22Rv1 cells. These results showed that SPOP also plays a role in regulating LIMK2, eliciting a negative feedback loop.

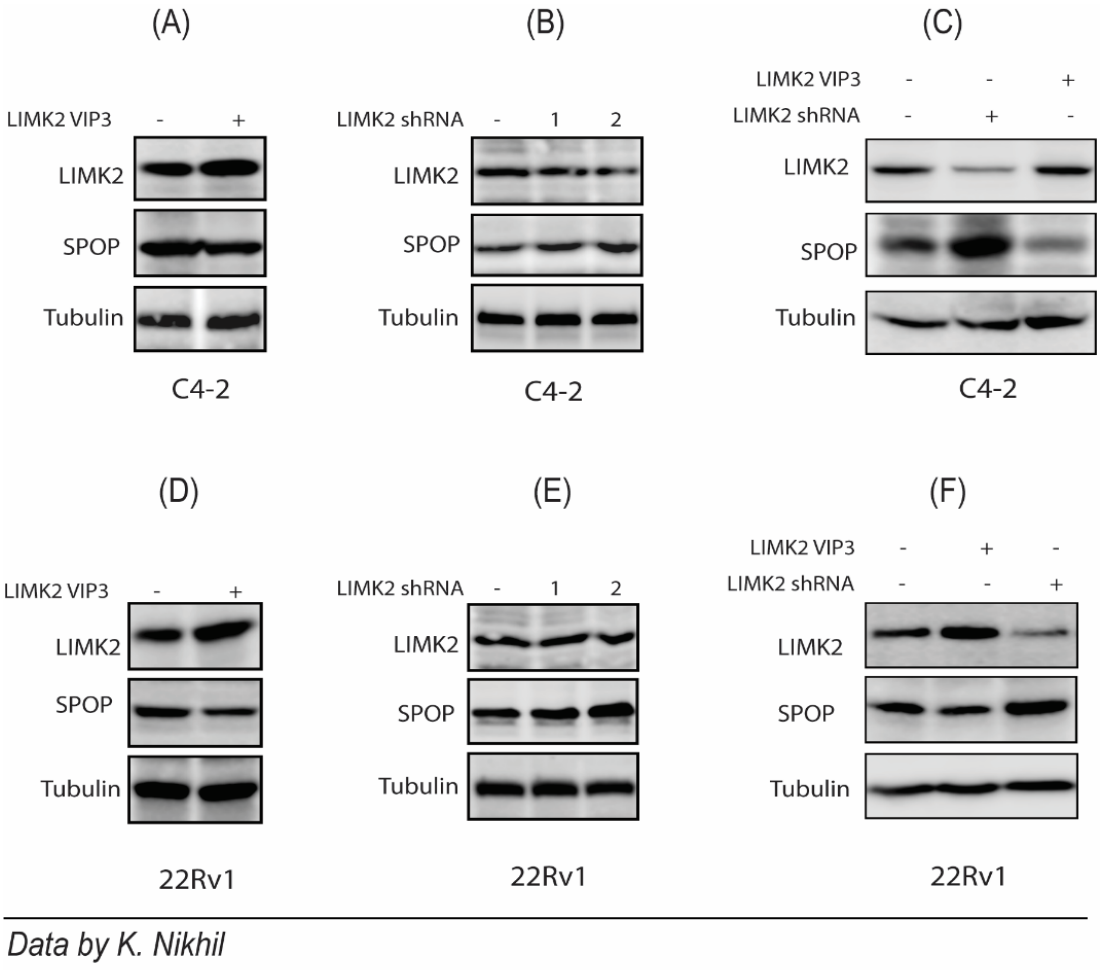

Figure 2.8 LIMK2 regulates SPOP protein level. (A) LIMK2 overexpression in C4-2 cells reduces the SPOP protein expression level. (B) The removal of LIMK2 using LIMK2-shRNA1 and LIMK2-shRNA2 elevates SPOP protein levels in C4-2 cells compared to control cells. (C) LIMK2 overexpression and LIMK2-removal are together compared to control cells. (D) LIMK2 overexpression in 22Rv1 cells decreases the SPOP protein expression level. (E) LIMK2 removal using LIMK2-shRNA1 and LIMK2-shRNA2 increases SPOP protein levels in 22Rv1 cells compared to control cells. (F) LIMK2 overexpression and LIMK2 removal in 22Rv1 cells is compared to control cells

2.2.3 LIMK2 directly phosphorylates SPOP

The above results encouraged us to investigate whether LIMK2 regulates SPOP directly via phosphorylation. For this, we cloned the 6x-His-SPOP into the TAT-HA vector at the BamHI and XhoI sites. The protein was expressed in BL21 competent cells and purified using Ni-NTA beads. More details about cloning, protein expression, and protein purification can be found in Chapter 5.

WT-SPOP was subjected to radioactive *in vitro* kinase assay using [γ-^{32}P] ATP in the presence of LIMK2 kinase. The amount of phosphorylation was quantified using autoradiography. In addition to WT-SPOP reactions with LIMK2, reactions of LIMK2 alone and WT-SPOP alone were used as controls. The results showed that LIMK2 robustly phosphorylates WT-SPOP (Figure 2.2).

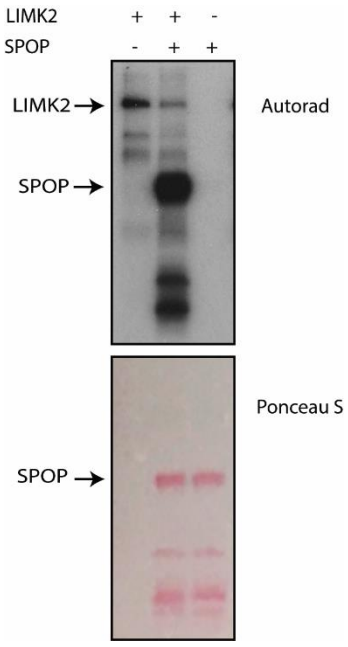

Figure 2.9 LIMK2 directly phosphorylates WT-SPOP. The first lane from the left is LIMK2 alone, the second lane is WT-SPOP with LIMK2, and the third lane is SPOP alone. All samples have a 10X kinase buffer, 0.5 µCi [γ-32P] ATP and DI-H_2O to adjust the reaction to a 25µL final scale.

The next step was to find the phosphorylation sites in SPOP. We found that cutting the protein into pieces would be useful in narrowing down the many possible sites of phosphorylation that we predicted. We therefore cut the protein into three parts and tested each one individually for phosphorylation by radioactive *in-vitro* kinase assay. Our result showed that two of the SPOP pieces where phosphorylated but not the third piece (Figure 2.4) for more details, see the SPOP Fragmentation section below.

2.2.4 SPOP Fragmentation

To narrow down the possibilities of the predicted phosphorylation sites, we cut WT- SPOP into three pieces as shown in Figure 2.3. Taking SPOP Domains into consideration, we cut the protein so that the first piece contained the MATH domain from the first amino acid to Lysine 180 (SPOP-1-180). The second piece contained the BTB domain from Valine 181 to glutamic acid 300 (SPOP-181-300), and the last piece, which included the C-terminal domain, contained the rest of the protein sequence from Asparagine 301 to the end (SPOP-301-374).

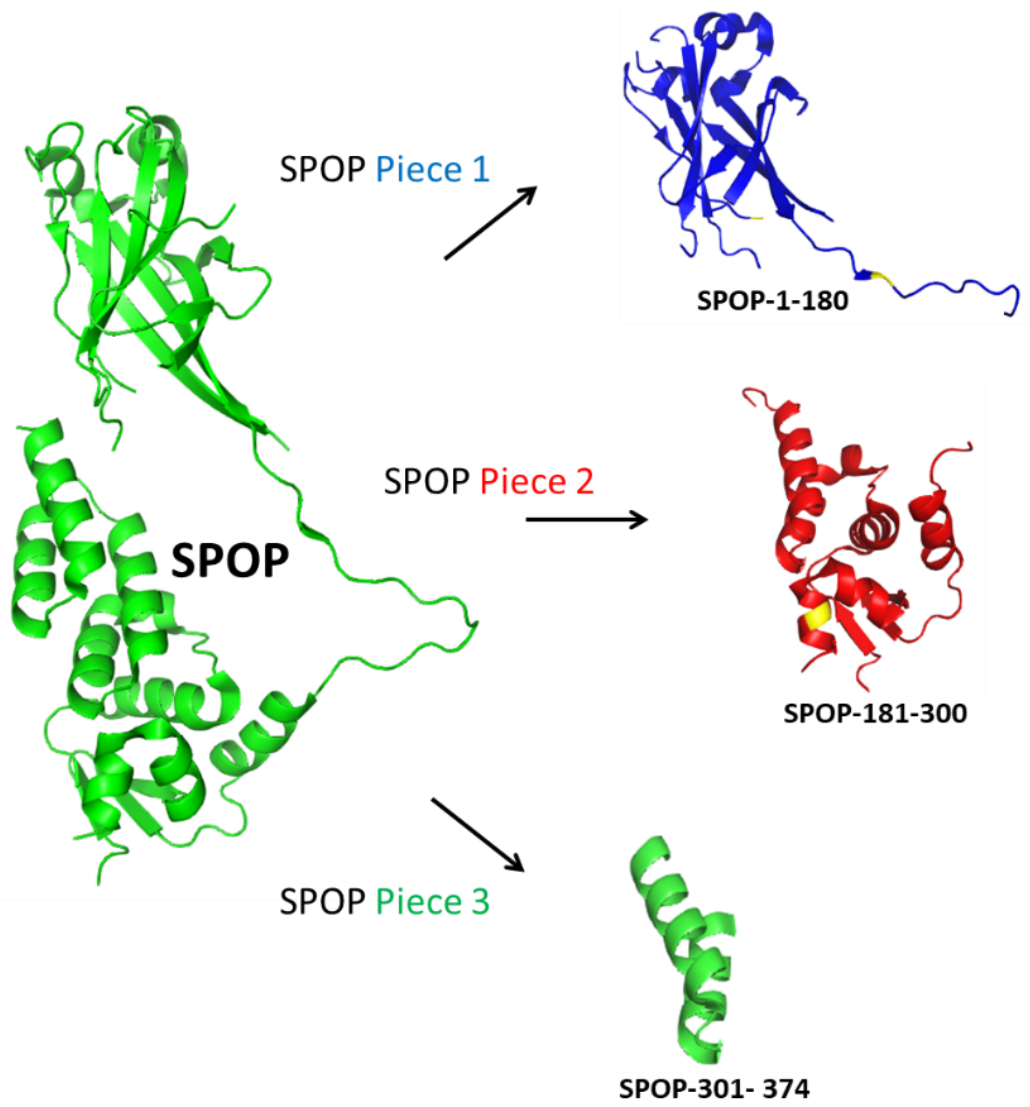

Figure 2.10 A crystallized structure of SPOP illustrates its fragmentation into three pieces: (Blue) SPOP-1-180 which contains the MATH domain, SPOP-1-180 was cloned into the TAT-HA vector at the BamHI and EcoRI sites; (Red) SPOP-181-300 which contains the BTB domain in SPOP, was cloned into the TAT-HA vector at the BamHI and XhoI sites; and (Green, the smaller piece in the figure) SPOP-301-374 in the C-terminus domain region, was cloned into the TAT-HA vector at the BamHI and XhoI sites. All SPOP-fragments are 6x-His tagged.

SPOP fragments were cloned into the TAT-HA vector at the BamHI and EcoRI sites for piece one (SPOP-1-180), and they were cloned into the BamHI and XhoI sites for pieces two and three (SPOP-181-300, SPOP-301-374) respectively. The primer sequences are included in Table 5.1 in Chapter 5. SPOP fragments were expressed in BL21 competent cells as mentioned previously in the methodology section and were identified based on the calculated size and western blotting of each one. Successfully, SPOP fragments were individually tested for phosphorylation by *in vitro* kinase assay with LIMK2. The results were positive for the first and the second SPOP-pieces, SPOP-1-180 and SPOP-181-300, and they were negative for the third piece SPOP-301-374 see (Figure 2.4).

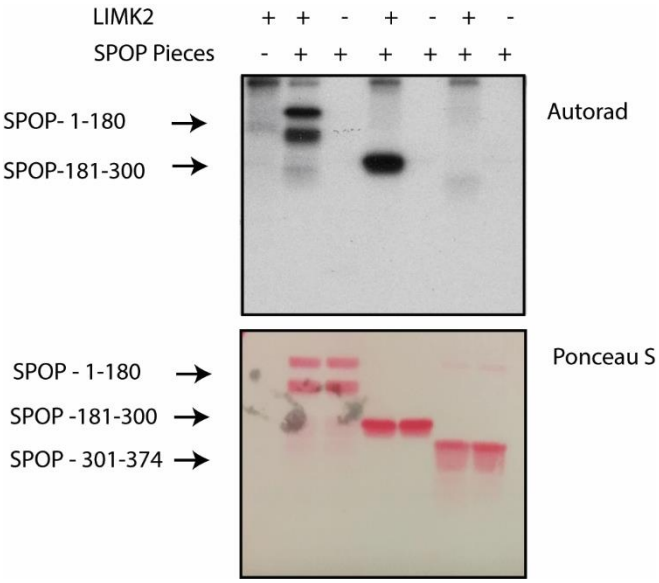

Figure 2.11 LIMK2 phosphorylates SPOP-1-180 and SPOP-181-300. The 1st line (L1) from the left is LIMK2 alone. (L2) is SPOP-1-180 with LIMK2, and (L3) is SPOP-1-180 alone. (L4) shows SPOP-180-300 with LIMK2, (L5) is SPOP-180-300 alone. (L6) is SPOP-301-374 with LIMK2, and (L7) SPOP-301-374 is alone. All samples have a 10X kinase buffer, 0.5 µCi [γ-32P] ATP and DI-H_2O to adjust the reaction to a 25µL final scale

2.2.5 Phosphorylation of SPOP on S59A, S171A, and S226A

Working in our laboratory (the Shah lab) we were able to predict the correct SPOP phosphorylation sites by LIMK2 with a good deal of success. Other studies have reported, alternately, that protein kinases recognize their substrates via docking interaction and the interaction near the phosphosite[10]. Yet another study showed that one LIMK2 family member, LIMK1, recognizes cofilin by docking interactions, but it does not have overall interactions with cofilin close to the phosphosite[11]. As discussed in a recent Shah lab publication[3], there is still no consensus regarding a favorable amino-acid sequence for the phosphorylation of LIMK2. Following the same strategy mentioned in this paper, we initially chose six serine sites that were followed by alanine or glycine as potential, predicted phosphorylation sites on SPOP. Those sites were the S59, S171, S226, S313, S336, and S358. We also suggested three other tyrosine sites, the Y259, Y280 and Y353, as weak possibilities for potential LIMK2 sites. Based on the protein fragmentation results shown in (Figure 2.4), we eliminated the last three potential serine sites, S313, S336, and S358, as well as one tyrosine site Y353. The SPOP potential sites S313, S336, and S358 are found in the last SPOP fragment (SPOP-301-374), which showed no phosphorylation (Figure 2.4). We also eliminated the remaining possible tyrosine sites, Y259 and Y280, based on a 4G10 tyrosine assays (data is not included here).

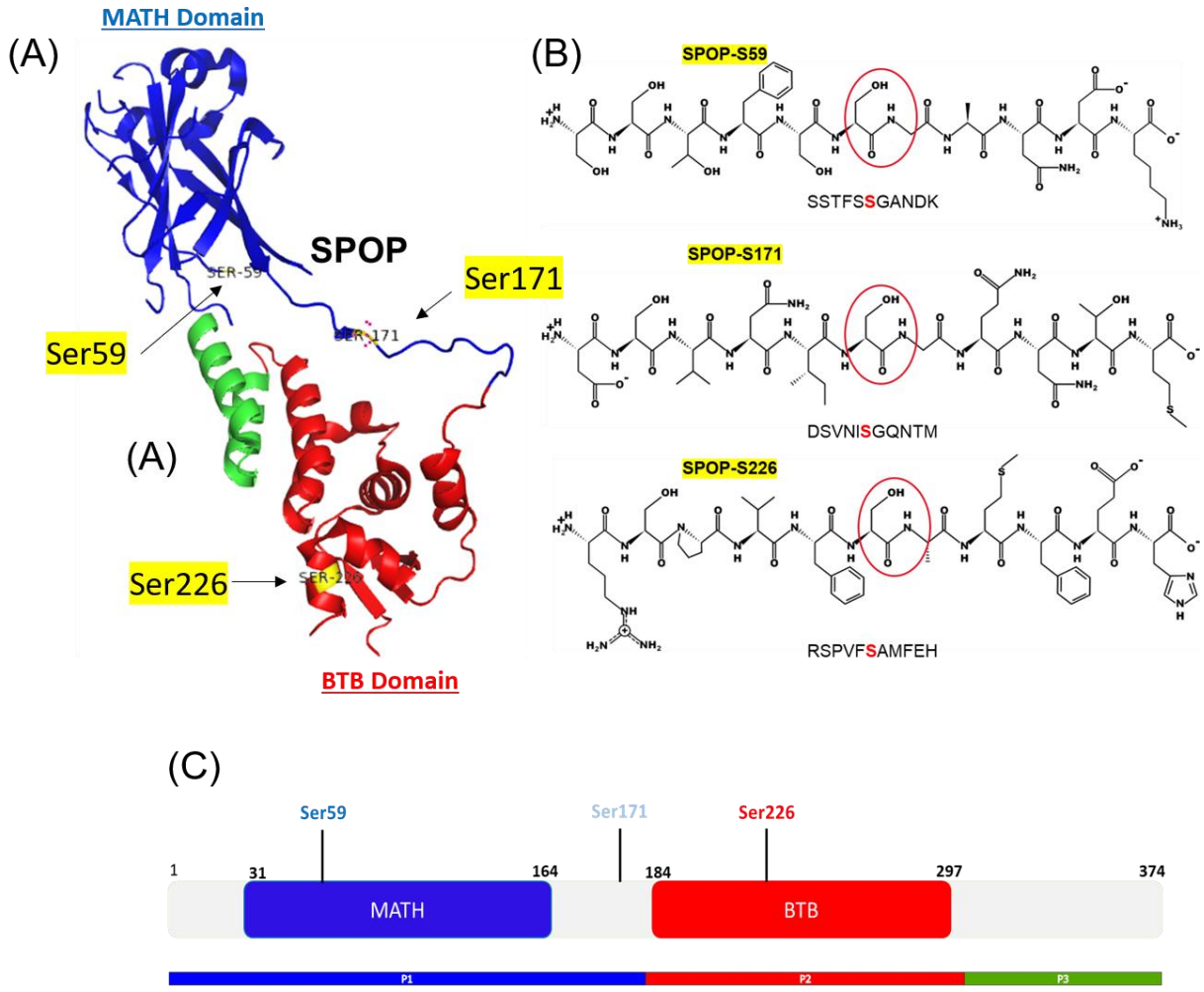

Figure 2.12 The identification of SPOP phosphorylation sites by LIMK2. (A) A crystal structure of SPOP illustrates the identified phosphorylation sites Ser59, Ser171 and Ser226, and their localization in these domains: the (Blue) SPOP-MATH domain, and (Red) SPOP-BTB domain. (B) The amino-acid residue sequence showing the SPOP-sites of phosphorylation by LIMK2 favoring a glycine or alanine followed the phosphorylation sites. (C) A representation of the SPOP structural domains, showing the SPOP phosphorylation sites by LIMK2 and its localization. P1, P2, and P3 are the original fragments generated to predict the phosphorylation sites.

The three potential remaining sites, S59, S171 and S226, were mutated individually using site-directed mutagenesis. All sites were mutated by changing the serine to alanine. The initial study on site 59 was done by mutating serine number 58 in combination with S59 by cloning a double mutant S58A and S59A. The reduction of phosphorylation observed in the mutant was confirmed by cloning S59A alone, which also confirmed that S59 is one of the phosphorylation sites, but not S58. We observed reduced phosphorylation in each mutant individually, and the lack of phosphorylation of the triple mutant SPOP-S59A, S171A, and S226A is shown in (Figure 2.6) and (Figure 2.7)

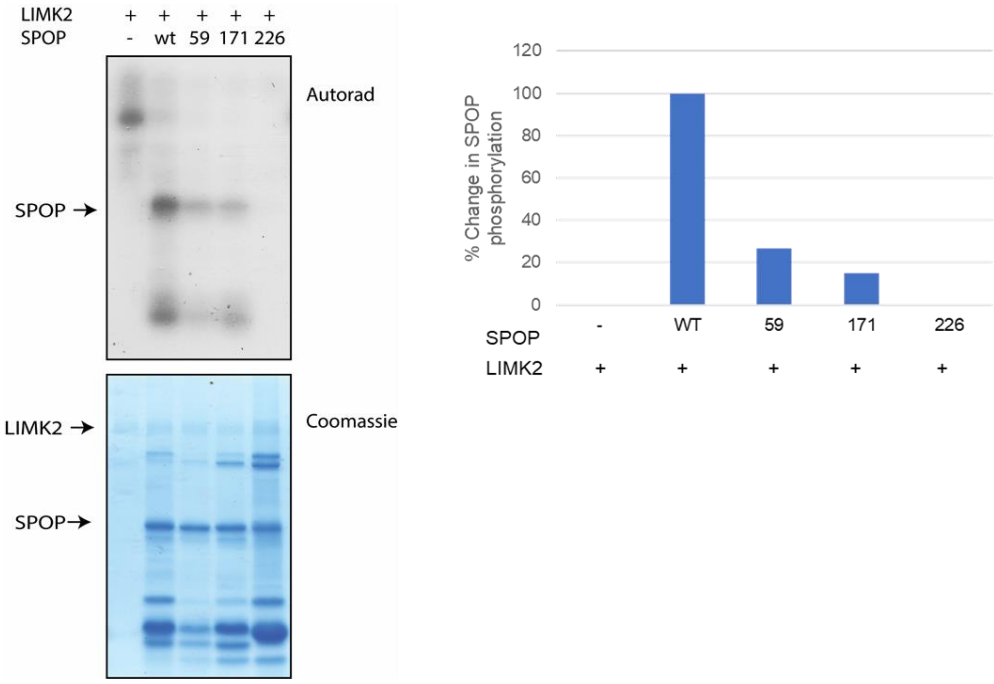

Figure 2.13 Phosphorylation reduction in SPOP mutants compared to WT-SPOP. LIMK2 phosphorylates SPOP at S59, S171, and S226. Lane 1 (L1) contains LIMK2 only(L2) contains WT-SPOP and LIMK2, (L3) contains SPOP-S59A mutant and LIMK2, (L4) contains SPOP-S171A mutant and LIMK2, (L5) contains SPOP-S226A mutant and LIMK2. All lanes also have, [^{32}P]ATP, 10X kinase buffer and DI-H_2O to adjust the reaction to 25µL final scale. Also, all SPOPs are 6x-His tagged. Kinase assay was conducted for 30 min. The Top panel shows autoradiography and the bottom panel shows LIMK2 and SPOPs coomassie blue stain. The mutants were generated and subjected to *in vitro* kinase assay using LIMK2. The bar graph shows the phosphor-resistant mutants of SPOP compare to WT-SPOP

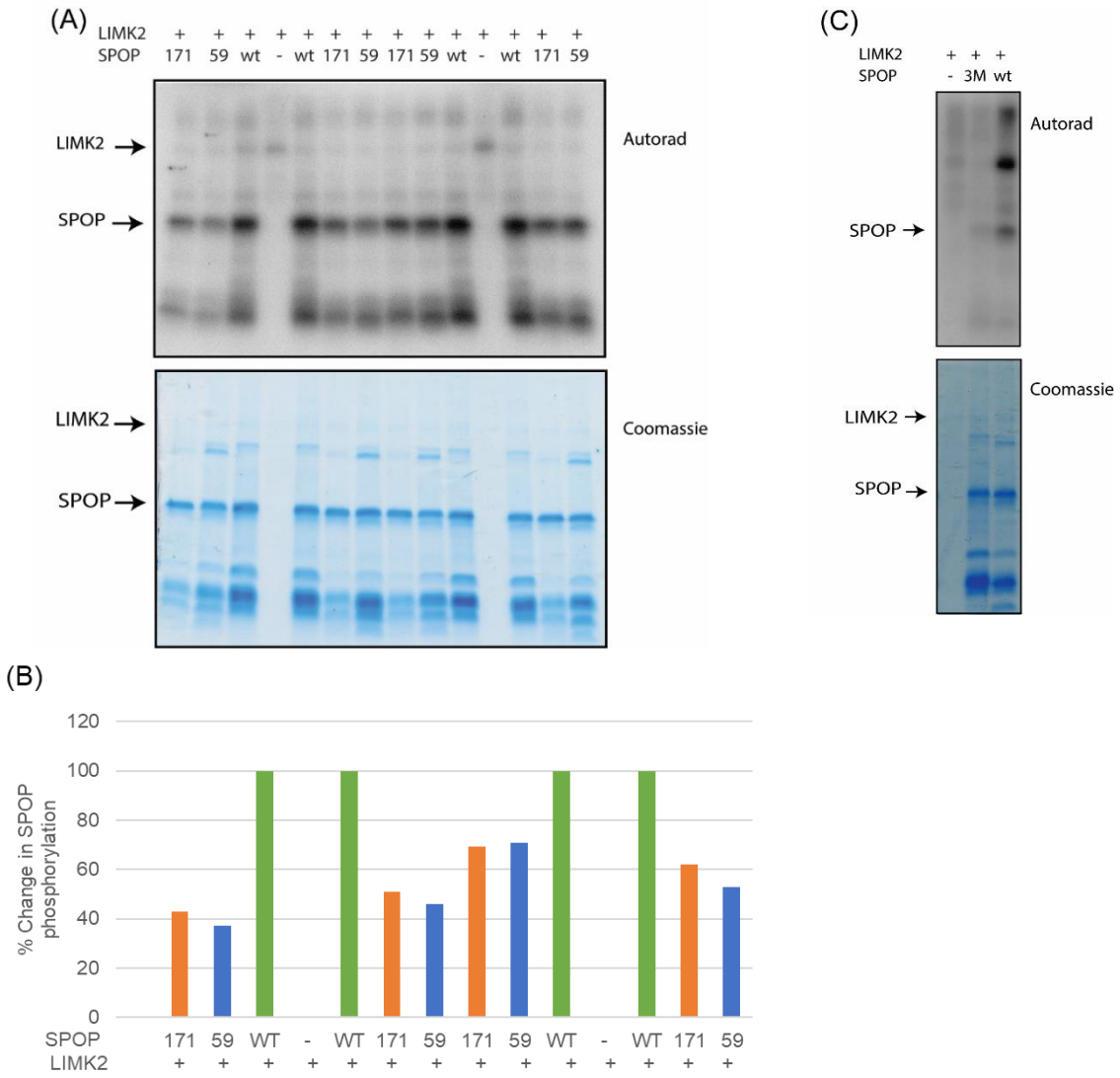

Figure 2.14 LIMK2 directly phosphorylates SPOP. (A) The top panel shows autoradiography and the bottom panel shows LIMK2 and SPOP's Coomassie blue stain. LIMK2 phosphorylates SPOP at S59, S171, and S226 (S226 is not shown in this experiment). Lane 1 (L1) contains SPOP-S171A mutant and LIMK2, (L2) contains SPOP-S59A mutant and LIMK2, (L3) contains WT-SPOP and LIMK2, (L4) contains LIMK2 only, (L5) contains WT-SPOP and LIMK2, (L6) contains SPOP-S171A mutant and LIMK2, (L7) contains SPOP-S59A mutant and LIMK2, (L8) contains SPOP-S171A mutant and LIMK2, (L9) contains SPOP-S59A mutant and LIMK2, (L10) contains WT-SPOP and LIMK2, (L11) contains LIMK2 only, (L12) contains WT-SPOP and LIMK2, (L13) contains SPOP-S171A mutant and LIMK2, (L14) contains SPOP-S59A mutant and LIMK2. All samples also have a [^{32}P]ATP, 10X kinase buffer. All SPOPs are 6x-His tagged. A kinase assay was conducted for 30 min. The mutants were generated and subjected to the *in vitro* kinase assay using LIMK2. (B) A bar graph shows the phosphor-resistant mutants of SPOP compare to WT-SPOP in four sets of experiments. (C) (L1) contains LIMK2 only, (L2) contains the SPOP-3M (S59A, S171A, and S226A) mutant and LIMK2, (L3) contains WT-SPOP and LIMK2. All lanes also contain a [^{32}P]ATP, 10X kinase buffer.

2.3 Discussion

LIMK2 is overexpressed in several human cancers. We showed that LIMK2 is upregulated in prostate cancer upon castration in mice and in human CRPC tissues[3]. Nearly one of five of men with metastatic prostate cancer develop castration-resistant prostate cancer, where the tumor cells become resistant to hormone therapy. To date, the molecular mechanism by which LIMK2 promotes tumorigenesis, angiogenesis, chemoresistance, tumor-cell migration and invasion remain unknown. Moreover, to date only three LIMK2 substrates have been identified. Discovering other substrates for LIMK2 is necessary for understanding the signaling pathways in which LIMK2 participates.

SPOP is among one of the most frequently mutated protein in prostate cancer[12]. In this study, we identified SPOP as a novel substrate for LIMK2.Cellularstudies from our lab showed that there is an inverse relationship between LIMK2 and SPOP in prostate cancer cells at the protein expression level, where overexpression of one of them reduces the protein expression of the other. These positive results encouraged us to investigate further what kind of post-translation-modification LIMK2 has on SPOP that leads to its negative regulation.

We found that LIMK2 directly phosphorylates SPOP at S59, S171, and S226. We started by truncating SPOP into three pieces to help us more quickly identify the phosphorylation sites of SPOP. Initially, we predicted nine possible phosphorylation sites on the SPOP sequence. However, fragmenting SPOP into three pieces reduced the possibilities from nine to three sites. LIMK2 phosphorylated the first and second truncated proteins (SPOP-1-180, and SPOP181-300), but not the last (SPOP-301-374). Finally, we focused on the remaining predicted sites, S59, S171 and S226. All three showed a reduction

in phosphorylation, but S226 appeared to be a better site, where some results showed slight phosphorylation and others showed no phosphorylation at all. The phosphorylation sites are localized in the MATH and BTB domains of SPOP, and these domains, as mentioned earlier, are involved in many essential functions that are needed to regulate SPOP's substrates, and to recruit its substrates for ubiquitination and protein degradation. Our finding that LIMK2 phosphorylates these two domains could be a strong lead for future studies to help us better understand why SPOP is mutated in prostate cancer. Targeting LIMK2 directly or indirectly through SPOP and its other substrates holds tremendous therapeutic potential in treating prostate cancer.

2.4 Material and Methods

2.4.1 Buffers

Most of the buffers used in these experiments (including the protein and kinase lysis buffers, DNA and protein purification buffers, kinase buffers etc.) were made in our laboratory. For more information, see buffer recipes in Chapter 5.

2.4.2 PCR Primers

All primers were ordered from Sigma Genosys. See Chapter 5, Table 5.1, for primer sequences.

2.4.3 SPOP Fragmentation

SPOP fragments were cloned into the TAT-HA vector at the BamHI and EcoRI sites for piece one (SPOP-1-180), and the BamHI and XhoI sites for pieces two and three (SPOP-181-300, SPOP-301-374) respectively. SPOP-fragments were expressed in BL21

competent cells as all were identified based on their calculated size and western blotting. All fragments were individually tested by kinase assay with LIMK2. For detailed procedures for cloning SPOP-fragments, their protein expression and purification procedures, we followed the general procedures described in Chapter 5.

2.4.4 Cloning and Site-Directed Mutagenesis

SPOP was cloned into the TAT-HA vector at the BamHI and XhoI sites, and SPOP mutants were generated using site-directed mutagenesis. For the primer sequence and other details, see Chapter 5.

2.4.5 Transformation and production of plasmid DNA

See the Methodology section in Chapter 5.

2.4.6 Bacterial Protein Expression and purification

6x-His-SPOP was expressed in BL21 *E. coli* competent cells and purified using a French press machine and Ni-NTA beads. SPOPs were expressed in BL21 competent cells and were confirmed using SPOP monoclonal antibodies. For more details, see Chapter 5.

2.5 References

1. Bach, I., The LIM domain: regulation by association. Mech Dev 2000, 91 (1-2), 5-17.

2. Scott, R. W.; Olson, M. F., LIM kinases: function, regulation and association with human disease. J Mol Med (Berl) 2007, 85 (6), 555-68.

3. Nikhil, K.; Chang, L.; Viccaro, K.; Jacobsen, M.; McGuire, C.; Satapathy, S. R.; Tandiary, M.; Broman, M. M.; Cresswell, G.; He, Y. J.; Sandusky, G. E.; Ratliff, T. L.; Chowdhury, D.; Shah, K., Identification of LIMK2 as a Therapeutic Target in Castration Resistant Prostate Cancer. Cancer Lett 2019.

4. Vardouli, L.; Moustakas, A.; Stournaras, C., LIM-kinase 2 and cofilin phosphorylation mediate actin cytoskeleton reorganization induced by transforming growth factor-beta. J Biol Chem 2005, 280 (12), 11448-57.

5. Johnson, E. O.; Chang, K. H.; Ghosh, S.; Venkatesh, C.; Giger, K.; Low, P. S.; Shah, K., LIMK2 is a crucial regulator and effector of Aurora-A-kinase-mediated malignancy. J Cell Sci 2012, 125 (Pt 5), 1204-16.

6. Lagoutte, E.; Villeneuve, C.; Lafanechère, L.; Wells, C. M.; Jones, G. E.; Chavrier, P.; Rossé, C., LIMK Regulates Tumor-Cell Invasion and Matrix Degradation Through Tyrosine Phosphorylation of MT1-MMP. Sci Rep 2016, 6, 24925.

7. Brenner, J. C.; Chinnaiyan, A. M., Disruptive events in the life of prostate cancer. Cancer Cell 2011, 19 (3), 301-3.

8. Barbieri, C. E.; Baca, S. C.; Lawrence, M. S.; Demichelis, F.; Blattner, M.; Theurillat, J. P.; White, T. A.; Stojanov, P.; Van Allen, E.; Stransky, N.; Nickerson, E.; Chae, S. S.; Boysen, G.; Auclair, D.; Onofrio, R. C.; Park, K.; Kitabayashi, N.; MacDonald, T. Y.; Sheikh, K.; Vuong, T.; Guiducci, C.; Cibulskis, K.; Sivachenko, A.; Carter, S. L.; Saksena, G.; Voet, D.; Hussain, W. M.; Ramos, A. H.; Winckler, W.; Redman, M. C.; Ardlie, K.; Tewari, A. K.; Mosquera, J. M.; Rupp, N.; Wild, P. J.; Moch, H.; Morrissey, C.; Nelson, P. S.; Kantoff, P. W.; Gabriel, S. B.; Golub, T. R.; Meyerson, M.; Lander, E. S.; Getz, G.; Rubin, M. A.; Garraway, L. A., Exome sequencing identifies recurrent SPOP, FOXA1 and MED12 mutations in prostate cancer. Nat Genet 2012, 44 (6), 685-9.

9. Geng, C.; He, B.; Xu, L.; Barbieri, C. E.; Eedunuri, V. K.; Chew, S. A.; Zimmermann, M.; Bond, R.; Shou, J.; Li, C.; Blattner, M.; Lonard, D. M.; Demichelis, F.; Coarfa, C.; Rubin, M. A.; Zhou, P.; O'Malley, B. W.; Mitsiades, N., Prostate cancer-associated mutations in speckle-type POZ protein (SPOP) regulate steroid receptor coactivator 3 protein turnover. Proc Natl Acad Sci U S A 2013, 110 (17), 6997-7002.

10. Goldsmith, E. J.; Akella, R.; Min, X.; Zhou, T.; Humphreys, J. M., Substrate and docking interactions in serine/threonine protein kinases. Chem Rev 2007, 107 (11), 5065-81.

11. Hamill, S.; Lou, H. J.; Turk, B. E.; Boggon, T. J., Structural Basis for Noncanonical Substrate Recognition of Cofilin/ADF Proteins by LIM Kinases. Mol Cell 2016, 62 (3), 397-408.

12. Boysen, G.; Rodrigues, D. N.; Rescigno, P.; Seed, G.; Dolling, D.; Riisnaes, R.; Crespo, M.; Zafeiriou, Z.; Sumanasuriya, S.; Bianchini, D.; Hunt, J.; Moloney, D.; Perez-Lopez, R.; Tunariu, N.; Miranda, S.; Figueiredo, I.; Ferreira, A.; Christova, R.; Gil, V.; Aziz, S.; Bertan, C.; de Oliveira, F. M.; Atkin, M.; Clarke, M.; Goodall, J.; Sharp, A.; MacDonald, T.; Rubin, M. A.; Yuan, W.; Barbieri,

C. E.; Carreira, S.; Mateo, J.; de Bono, J. S., SPOP-Mutated/CHD1-Deleted Lethal Prostate Cancer and Abiraterone Sensitivity. Clin Cancer Res 2018, 24 (22), 5585-5593.

CHAPTER 3. SPOP IS A DIRECT SUBSTRATE FOR AURKA

3.1 Introduction

Aurora A kinase (AURKA) is a highly conserved serine/threonine kinase. It plays critical roles in regulating cancer cells by supporting the cell cycle progression and tumor development[1]. AURKA is a well-established oncogenic target that was found to be overexpressed in many types of cancer. It is specifically considered one of the biomarkers in prostate cancer[2]. Direct inhibition of AURKA can be lethal, which restricts its therapeutic potential in treating cancer[3]. Identification of AURKA substrates is critical in order to uncover its signaling pathways and to understand how to target AURKA without any resulting toxicity. Although the role of AURKA in the cell cycle is well established, its mechanism of action is not fully elucidated. Despite several known substrates for AURKA, the door for identifying more substrates in order to uncover its many functions is still open.

In this study, we found that the Speckle-type POZ protein (SPOP) is a direct substrate for AURKA.

3.2 Results

3.2.1 AURKA and SPOP regulation relationship

A previous study conducted in our lab showed that the overexpression of AURKA reduced the protein expression of wild type SPOP (WT-SPOP) in C4-2 prostate cancer cell lines. The knockdown of AURKA produced the opposite effect, a finding that showed SPOP to be negatively regulated at the protein level by AURKA. Similarly,

SPOP overexpression reversed the expression of AURKA, while SPOP knockdown increased the level of AURKA protein. This result indicates that AURKA and SPOP regulate each other in a negative feedback loop.

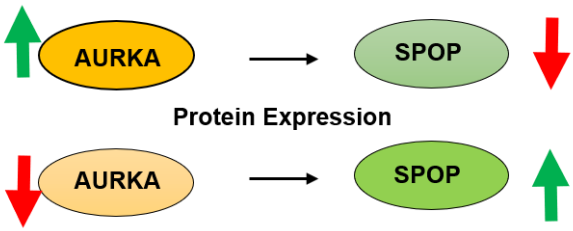

3.2.2 AURKA binds SPOP associates with each other

A previous experiment was performed in our lab to detect whether AURKA and SPOP interact with each other in the C4-2 cell. A co-immunoprecipitation (IP) assay using an AURKA antibody and SPOP antibody was used, followed by western blot analysis. The result confirmed that both these proteins interact with each other in C4-2 cancer cells. As mentioned earlier, the MATH domain of SPOP recruits proteins and kinases through binding, which affects their ability to control cell survival, proliferation, and death signaling[4] (for more details, see Chapter 1). Additionally, all SPOP mutations in prostate cancer are in the MATH domain[5]. In the next part of our study, we wanted to see whether interaction between AURKA and SPOP leads to SPOP phosphorylation, thus affecting the downstream signaling pathways.

3.2.3 AURKA directly phosphorylates SPOP

The above results led us to investigate whether AURKA regulates SPOP directly via phosphorylation. To do this, we cloned 6x-His-SPOP into the TAT-HA vector at the BamHI and XhoI sites. The protein was expressed in BL21 competent cells and purified using Ni-NTA beads. More details about cloning, protein expression, and protein purification can be found in Chapter 5.

WT-SPOP was subjected to radioactive *in vitro* kinase assay using 0.5 µCi of [γ-^{32}P] ATP in the presence of AURKA after its activation by TPX2. The amount of phosphorylation was quantified using autoradiography. In addition to WT-SPOP reaction with AURKA, AURKA alone and WT-SPOP alone reactions were used as controls. The results showed that AURKA phosphorylated WT-SPOP when it reacted with AURKA, while no signal was present in the SPOP alone sample which served as a negative control.

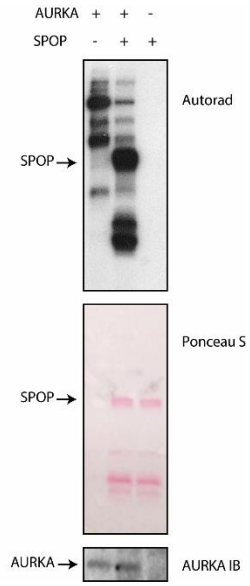

Figure 3.15 AURKA directly phosphorylates WT-SPOP. The first lane is AURKA alone, the second lane is WT-SPOP with AURKA, and the third lane is SPOP alone. All samples have a 10X kinase buffer, 0.5 µCi [γ-32P] ATP and DI-H2O to adjust the reaction to a 25µL final scale.

3.2.4 Predicting SPOP phosphorylation sites by Aurora A kinase

AURKA only phosphorylates serine and/or threonine amino acids, and it also prefers substrates with a special sequence. This was elucidated in a study where synthetic peptides derived from a phosphate acceptor peptide (Kemptide,) and other peptides, were screened using human Aurora A that was expressed in *E.coli*. The study defined the sequence recognized by Aurora A, explaining the positivity and negativity of the local features of the consensus sequence[6]. They concluded that the consensus sequence of Aurora A can be mapped as R/K/N-R-X-S/T-B, where B represents any hydrophobic residue other than Proline[6]. Using these findings as a starting point, we predicted three possible phosphorylation sites in SPOP, all found on the MATH domain of SPOP, Ser33, Thr56 and Ser105.

3.2.5 Aurora A phosphorylates SPOP-MATH Domain

The known substrate specificity of AURKA led us to successful prediction sites in SPOP. The three predicated phosphorylation sites, serine 33, threonine 56 and serine 105, were all followed by hydrophobic residues. To confirm that these sites are the kinase-phosphorylated sites, we single-mutated each site by changing serine and threonine to alanine. SPOP mutants S33A, T56A and S105A were subjected to in-vitro kinase assay, and we confirmed the reduction in phosphorylation compared to the WT-SPOP. (Figure 3.3). A double mutant of S33 and S105 was also generated by substituting both residues by alanine. We wanted to eliminate T56 from the list of predicted sites at the beginning because of its inconclusive data and the almost complete reduction of phosphorylation we found in the double mutant. T56A repeatedly showed a slight reduction in phosphorylation

compared to WT-SPOP, a finding that we could not ignore. Consequently, we generated a triple mutant of SPOP in all predicted sites by changing the residues from serine and threonine to alanine, and we performed *in vitro* kinase assay using the activated AURKA.

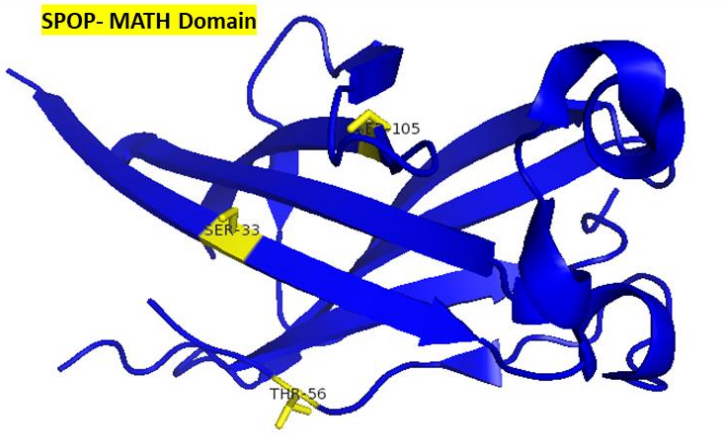

Figure 3.16 SPOP phosphorylation sites by AURKA are clustered in the MATH domain. AURKA directly phosphorylates SPOP at the sites Ser33, Thr56 and Ser105, and all sites localizae in the MATH domain**.** The phosphorylated sites are marked in yellow color.

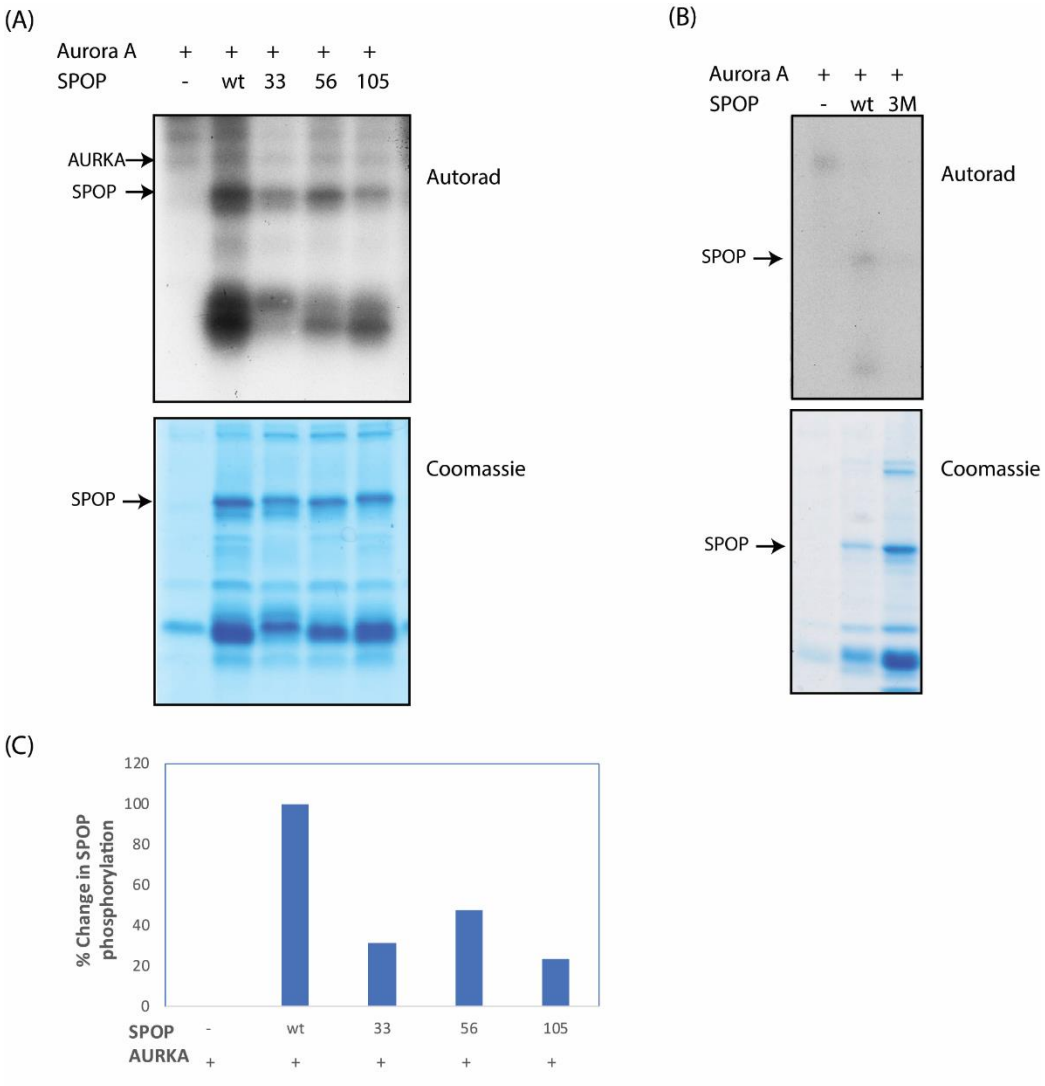

Figure 17.3 Phosphorylation reduction in SPOP mutants compared to WT-SPOP. AURKA phosphorylates SPOP at S33, T56, and S105. (A) Lane 1 (L1) contains AURKA only, (L2) contains WT-SPOP and AURKA, (L3) contains the SPOP-S33A mutant and AURKA, (L4) contains the SPOP-T56A mutant and AURKA, (L5) contains the SPOP-S105A mutant and AURKA. All lanes also contain a [^{32}P]ATP, 10X kinase buffer and DI-H_2O to adjust the reaction to a 25µL final scale. Noted also, all SPOPs are 6x-His tagged. A kinase assay was conducted for 30 min. (B) (L1) contains AURKA only, (L2) contains WT-SPOP and AURKA, (L3) contains the SPOP-3M (S33A, T56A, and S105) mutant and AURKA. All lanes also contain a [^{32}P]ATP, 10X kinase buffer and DI-H_2O to adjust the reaction to a 25µL final scale. All SPOPs are 6x-His tagged. A kinase assay was conducted for 30 min.(C) Bar graph shows the phosphor-resistant individual mutants of SPOP compared to WT-SPOP.

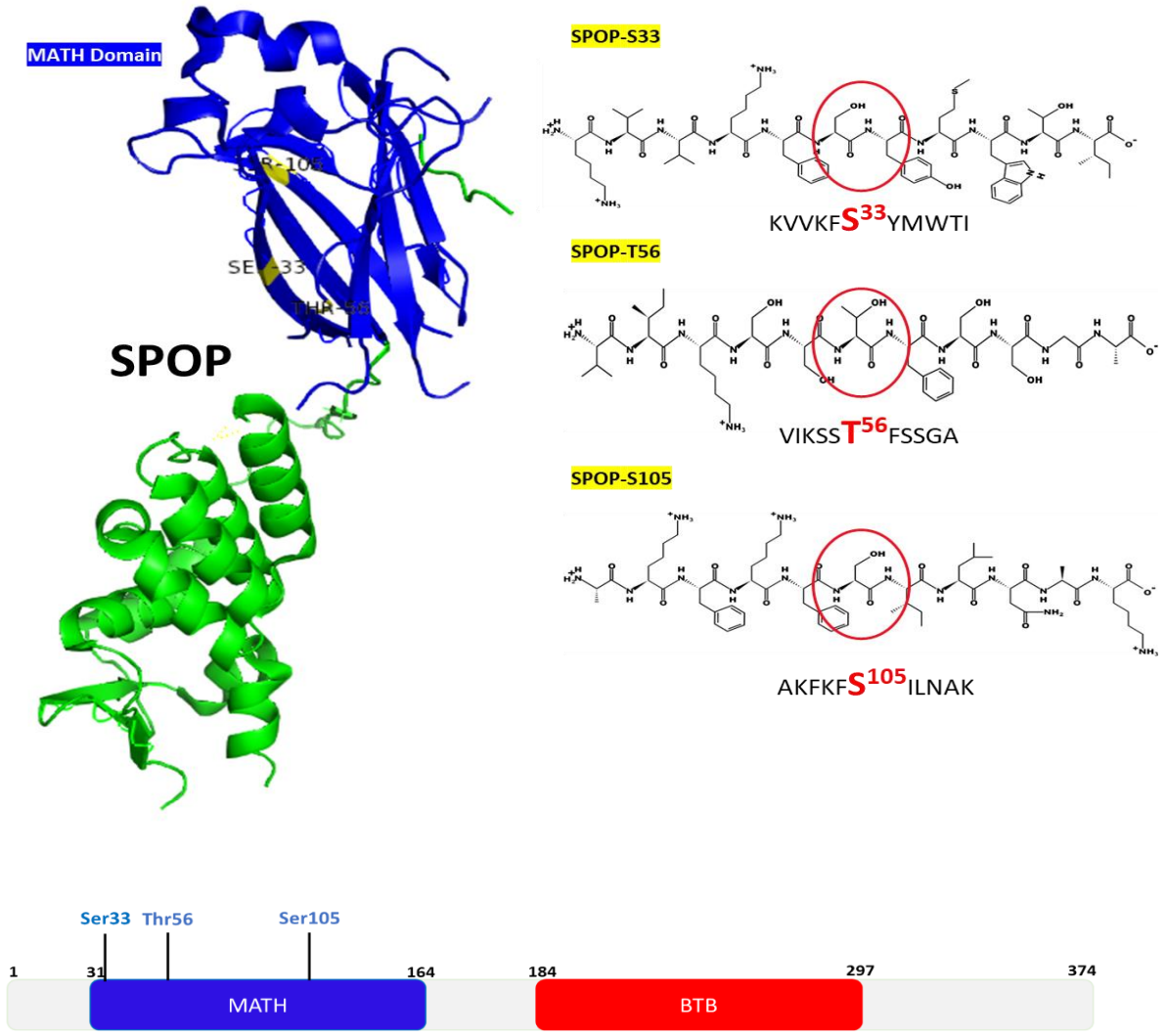

Figure 3.18 The identification of SPOP phosphorylation sites by AURKA. (Left side) a crystal structure of SPOP illustrates the identified phosphorylation sites Ser33, Thr56 and Ser105, and their localization in the MATH domain. (Right side) is the amino-acid sequence recognized by AURKA, where the residue following the site of phosphorylation is hydrophobic. The phosphorylation sites of SPOP by AURKA are circled.

3.3 Discussion

As discussed earlier, Aurora A kinase (AURKA) is a serine/threonine kinase which plays critical roles in regulating cancer cells by supporting the cell cycle progression and tumor development[1]. AURKA is a well-established oncogenic target and is overexpressed in many types of cancer, and it is specifically considered one of the biomarkers in prostate cancer[2]. Since the inhibition of AURKA can be lethal, this restricts its therapeutic potential[3].

In this study, we found that the Speckle-type POZ protein (SPOP) is a direct substrate for AURKA. AURKA phosphorylates SPOP at three sites within the MATH (meprin and TRAF-homology) domain. The MATH N-terminal domain of SPOP is known to be the most important part of SPOP that assists in recruiting proteins and kinases for ubiquitination and protein degradation [4, 7, 8]. Almost all reported SPOP mutations in cancer are found in the MATH domain of SPOP[8]. MATH phosphorylation must be an important post-translational modification to SPOP considering that it leads its regulation. Our results were supported by initial studies in C4-2 and 22Rv1 prostate cancer cells, which showed that AURKA negatively regulates SPOP at the protein expression level. A previous study in our lab also showed that AURKA binds to SPOP and cause its degradation (data is not included here). Subsequently, we identified the SPOP/AURKA phosphorylation sites using site-directed mutagenesis, a method that involves mutating the predicted sites and looking for the reduction in phosphorylation.

As mentioned earlier, AURKA only phosphorylates serine and/or threonine amino acids, and prefers substrates with a special sequence mapped as R/K/N-R-X-S/T-B, where B represents a hydrophobic residue[6]. Following this map, we hypothesized that AURKA phosphorylates SPOP on Ser33, Thr56 and Ser105. To prove our hypothesis, we mutated

each residue individually, creating a single mutant of S33A, T56A and S105A. Consequently, we generated a triple mutant of SPOP by changing the residues from serine and threonine to alanine. We cloned the mutated genes, expressed the protein and performed an *in vitro* kinase assay. S33A and S105 showed the maximum reduction in phosphorylation which was approximately 70% and 75% respectively, compared to WT-SPOP, while T56A showed about a 50% reduction in phosphorylation compared to WT-SPOP (Figure 3.3, A and C). The triple mutant (3M) showed almost no phosphorylation compared to WT-SPOP (Figure 3.3, B and D). Our results confirm that AURKA phosphorylates SPOP at S33, T56 and S105 only. These results indicate SPOP as a novel substrate for AURKA.

3.4 Material and Methods

3.4.1 Buffers

Most of the buffers used in our experiments (this includes the protein and kinase lysis buffers, DNA and protein purification buffers, kinase buffers, etc.) were made in our laboratory. See buffer recipes in Chapter 5.

3.4.2 PCR Primers

All primers were ordered from Sigma Genosys. See Chapter 5, Table 5.1 for primer sequences.

3.4.3 Cloning and Site-Directed Mutagenesis

SPOP was cloned into the TAT-HA vector at the BamHI and XhoI sites. SPOP mutants were generated using site-directed mutagenesis. For the primer sequence and other details, see Chapter 5.

3.4.4 Transformation and production of plasmid DNA

For information on the methodology, see Chapter 5.

3.4.5 Bacterial Protein Expression and purification

6x-His-SPOP was expressed in BL21 *E. coli* competent cells and purified using a French press machine and Ni-NTA beads. SPOPs were expressed in BL21 competent cells and were confirmed using SPOP monoclonal antibodies. For more details, see Chapter 5.

3.4.6 Sf9 cell protein expression and purification

AURKA was expressed and in Sf9 cells. Procedure details for purifying the kinase can be found in Chapter 5.

3.5 References

1. Tang, A.; Gao, K.; Chu, L.; Zhang, R.; Yang, J.; Zheng, J., Aurora kinases: novel therapy targets in cancers. Oncotarget 2017, 8 (14), 23937-23954.

2. Kivinummi, K.; Urbanucci, A.; Leinonen, K.; Tammela, T. L. J.; Annala, M.; Isaacs, W. B.; Bova, G. S.; Nykter, M.; Visakorpi, T., The expression of AURKA is androgen regulated in castration-resistant prostate cancer. Sci Rep 2017, 7 (1), 17978.

3. Lu, L. Y.; Wood, J. L.; Ye, L.; Minter-Dykhouse, K.; Saunders, T. L.; Yu, X.; Chen, J., Aurora A is essential for early embryonic development and tumor suppression. J Biol Chem 2008, 283 (46), 31785-90.

4. Takahashi, I.; Kameoka, Y.; Hashimoto, K., MacroH2A1.2 binds the nuclear protein Spop. Biochim Biophys Acta 2002, 1591 (1-3), 63-8.

5. Barbieri, C. E.; Baca, S. C.; Lawrence, M. S.; Demichelis, F.; Blattner, M.; Theurillat, J. P.; White, T. A.; Stojanov, P.; Van Allen, E.; Stransky, N.; Nickerson, E.; Chae, S. S.; Boysen, G.; Auclair, D.; Onofrio, R. C.; Park, K.; Kitabayashi, N.; MacDonald, T. Y.; Sheikh, K.; Vuong, T.; Guiducci, C.; Cibulskis, K.; Sivachenko, A.; Carter, S. L.; Saksena, G.; Voet, D.; Hussain, W. M.; Ramos, A. H.; Winckler, W.; Redman, M. C.; Ardlie, K.; Tewari, A. K.; Mosquera, J. M.; Rupp, N.; Wild, P. J.; Moch, H.; Morrissey, C.; Nelson, P. S.; Kantoff, P. W.; Gabriel, S. B.; Golub, T. R.; Meyerson, M.; Lander, E. S.; Getz, G.; Rubin, M. A.; Garraway, L. A., Exome sequencing identifies recurrent SPOP, FOXA1 and MED12 mutations in prostate cancer. Nat Genet 2012, 44 (6), 685-9.

6. Ferrari, S.; Marin, O.; Pagano, M. A.; Meggio, F.; Hess, D.; El-Shemerly, M.; Krystyniak, A.; Pinna, L. A., Aurora-A site specificity: a study with synthetic peptide substrates. Biochem J 2005, 390 (Pt 1), 293-302.

7. Zhuang, M.; Calabrese, M. F.; Liu, J.; Waddell, M. B.; Nourse, A.; Hammel, M.; Miller, D. J.; Walden, H.; Duda, D. M.; Seyedin, S. N.; Hoggard, T.; Harper, J. W.; White, K. P.; Schulman, B. A., Structures of SPOP-substrate complexes: insights into molecular architectures of BTB-Cul3 ubiquitin ligases. Mol Cell 2009, 36 (1), 39-50.

8. Mani, R. S., The emerging role of speckle-type POZ protein (SPOP) in cancer development. Drug Discov Today 2014, 19 (9), 1498-502.

CHAPTER 4. YBX1 IS A DIRECT SUBSTRATE OF AURKA

4.1 Introduction

Aurora A kinase (AURKA) is a serine/threonine kinase that regulates certain aspects of mitosis. AURKA is known to be up-regulated in most types of cancer, including prostate cancer[1] as mentioned in Chapter 1. AURKA inhibition suppresses tumor growth and enhances chemosensitivity underscoring its critical role in PCa. Despite these encouraging findings, AURKA inhibition in Phase II clinical trials has been associated with several adverse side effects, suggesting that collateral inhibition of AURKA in rapidly proliferating normal tissues is responsible for the undesirable side effects. Therefore, finding a way to indirectly target AURKA could contribute significantly in combating collateral toxicity and development of novel cancer therapy[2].

Y-box binding protein (YBX1) is a multifunctional DNA/RNA binding protein with three functional domains that regulates and controls transcription and translation in normal cells[3]. YBX1 is a member of the cold−shock protein domain superfamily, which is important in cell development in all type of cells through its binding to nucleic acids and other proteins. It is well known that YBX1 is strongly involved in cancer progression[4-7].

Several phosphorylation sites have been reported on the YBX1 protein. One of these sites is the phosphorylation site at Ser165, which was found to be critical for the activation of the famous nuclear factor kB (NFkB)[3]. However, not many YBX1 phosphorylation sites have been reported in the CSD, despite reports that YBX1 is directly integrated with the cap-structure of the mRNA and regulated by the phosphorylation of Ser102 in the cold shock domain (CSD)[8]. Phosphorylation sites like Ser102, S165 and other modifications

illustrate that YBX1 can be regulated by post-translational modification in promoting cell proliferation and cancer growth[9].

YBX1 has been mapped in several studies with its aniline/proline rich N-terminal domain, the cold shock domain CSD, and the C-terminal tail domain. Out of all of these domains, CSD is the only solved structure to date, due to its instability[7, 10]. CSD is built from a beta-barrel structure, which is known to be highly conserved[10]. The CSD spans from residue 51 to residue 129, as shown in (Figure 4.1)

Here, we identified YBX1 as a novel direct substrate of AURKA. We also identified two new sites of phosphorylation in CSD of YBX1, which were phosphorylated by AURKA.

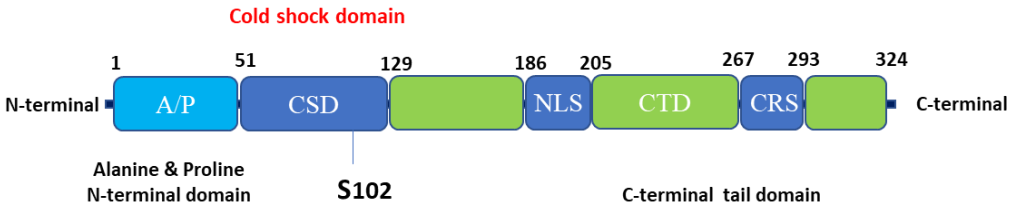

Figure 4.19 YBX1 structure and domains. YBX1 contains aniline/proline rich N-terminal domain, the cold shock domain CSD, and the C-terminal tail domain. Serine 102 (S102) is the first phosphorylation site identified for YBX1 in the CSD region.

4.2 Results

4.2.1 Aurora A kinase regulates YBX1 at the protein expression level

A previous study conducted in our lab showed that the overexpression of AURKA elevates the protein expression of YBX1 in C4-2 prostate cancer cell lines. The knockdown of AURKA using AURKA-shRNA showed opposite effects. Similarly, we found that YBX1 overexpression increased the expression of AURKA, while the knock down of YBX1

reduced the protein level of the AURKA protein. These results indicate that AURKA and YBX1 regulate each other.

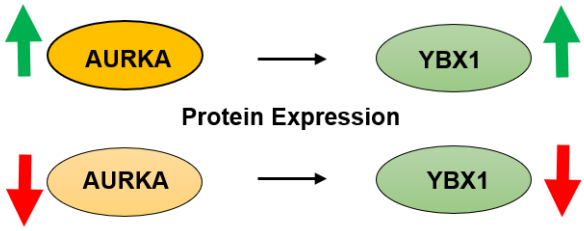

4.2.2 AURKA and YBX1 associate with each other

A previous experiment was performed in our lab to detect whether AURKA and YBX1 interact with each other in the C42 cell. A co-immunoprecipitation (IP) assay using an AURKA antibody and YBX1 antibody was used, followed by western blot analysis. The results confirmed that both these proteins interact with each other in C4-2 cancer cells. In the next part of our study, we wanted to see if interaction between AURKA and YBX1 leads to YBX1 phosphorylation, thus affecting the downstream signaling pathways.

4.2.3 YBX1 is directly phosphorylated by AURKA

In the course of our study, we wanted to learn whether or not AURKA regulated YBX1 at a post-translational state via phosphorylation. To answer this question, we cloned 6x-His-YBX1 into the TAT-HA vector at the BamHI and XhoI sites. The protein was expressed in BL21 competent cells and purified as mentioned in Chapter 5. Following this procedure, we subjected YBX1 to *in vitro* kinase assay by using 0.5 µCi of [γ-^{32}P] ATP in the presence of AURKA and TPX2. The amount of phosphorylation was quantified using

autoradiography. Since we know that YBX1 contains the favorable sequence of Aurora A for phosphorylation, we were anticipating positive results. The answer was clear as shown in the (Figure 4.2): Aurora A is directly phosphorylating YBX1.

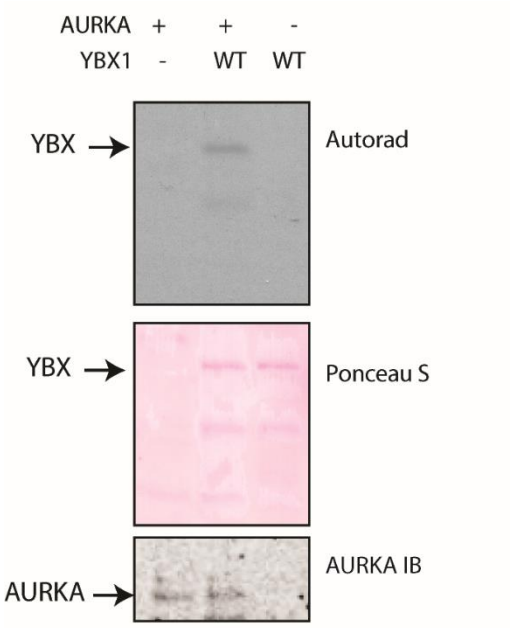

Figure 4.20 AURKA directly phosphorylates WT-YBX1. The first lane is AURKA alone, the second lane is WT-YBX1 with AURKA, and the third lane is YBX1 alone. All samples have a 10X kinase buffer, 0.5 μCi [γ-32P] ATP and DI-H2O to adjust the reaction to a 25μL final scale.

4.2.4 Predicting YBX1 phosphorylation sites by Aurora A kinase

As noted earlier, Aurora A prefers to phosphorylate R/K/N-**R**-X-S/T-**B**, where B represents any hydrophobic residue except for proline[11]. Based on these findings, we predicted two possible phosphorylation sites in YBX1, both found in the CSD domain of YBX1, Thr62 and Ser102.

4.2.5 Aurora A phosphorylates YBX1 on T62A, S102A sites

The known substrate specificity of Aurora A kinase led us to predict phosphorylation sites on YBX1. The predicated phosphorylation sites Thr62 and Ser102 were both followed by hydrophobic residues after phosphorylation. Surprisingly, other studies found the Ser102 residue of YBX1 to be phosphorylated after treatment of the insulin growth factor[5]. Additionally, mutating S102 of YBX1 was found to have a positive impact on reducing tumor growth in breast cancer. These results suggest that phosphorylation at S102 plays a critical oncogenic role[9].

To confirm our hypothesis and investigate that Thr62 and Ser102 are the sites phosphorylated by the kinase, we mutated each site individually by substituting serine and threonine with alanine. YBX1 mutants T62A and S102A were subjected to *in vitro* kinase assay and we confirmed the reduction in phosphorylation compared to WT-YBX1. (Figure 4.3) A double mutant of Thr62 and Ser102 was generated as well by changing both residues to alanine. Performing a kinase assay resulted in the total reduction of phosphorylation in the double mutant, suggesting that these are the only phosphorylation sites targeted by AURKA. (Figure 4.3)

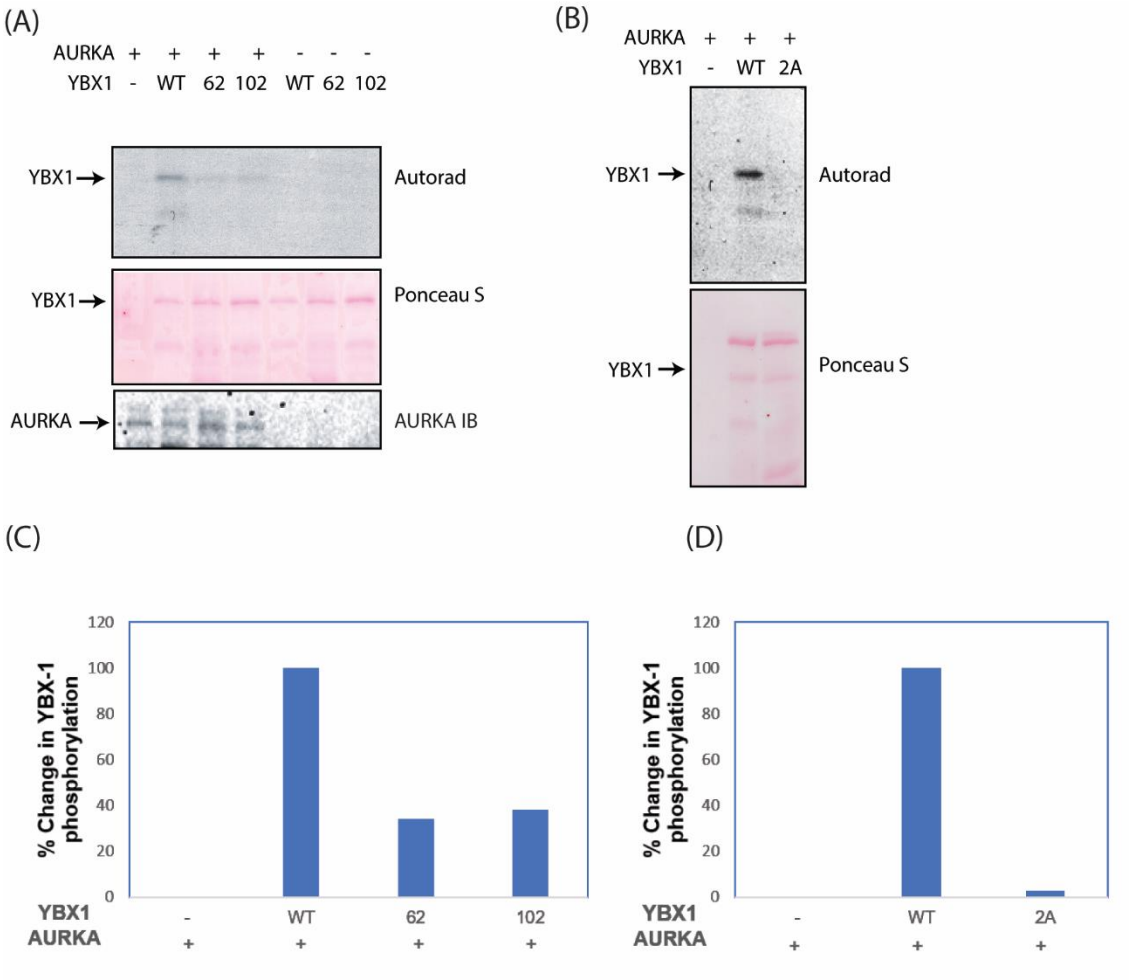

Figure 4.21 Phosphorylation reduction in YBX1 mutants compared to WT-YBX1. AURKA phosphorylates YBX1 at S62 and S102. (A) Lane 1 (L1) contains AURKA only, (L2) contains WT-YBX1 and AURKA, (L3) contains the YBX1-S62A mutant and AURKA, (L4) contains the YBX1-S102A mutant and AURKA, (L5) contains WT-YBX1 only, (L6) contains YBX1-S62A only, and (L7) contains YBX1-S102A only. All lanes also contain a [^{32}P]ATP, 10X kinase buffer and DI-H_2O to adjust the reaction to a 25µL final scale. Noted also, all YBXs are 6x-His tagged. A kinase assay was conducted for 30 min. (B) (L1) contains AURKA only, (L2) contains WT-YBX1 and AURKA, (L3) contains the YBX1-2A (S62A and S102A) mutant and AURKA. All lanes also contain a [^{32}P]ATP, 10X kinase buffer and DI-H_2O to adjust the reaction to a 25µL final scale. All SPOPs are 6x-His tagged. A kinase assay was conducted for 30 min. (C) Bar graph shows the phospho-levels of WT and phospho-resistant single mutant of YBX1 (D) Bar graph shows that the phospho-levels of WT and phospho-resistant double mutant (S62 and S102) of YBX1.

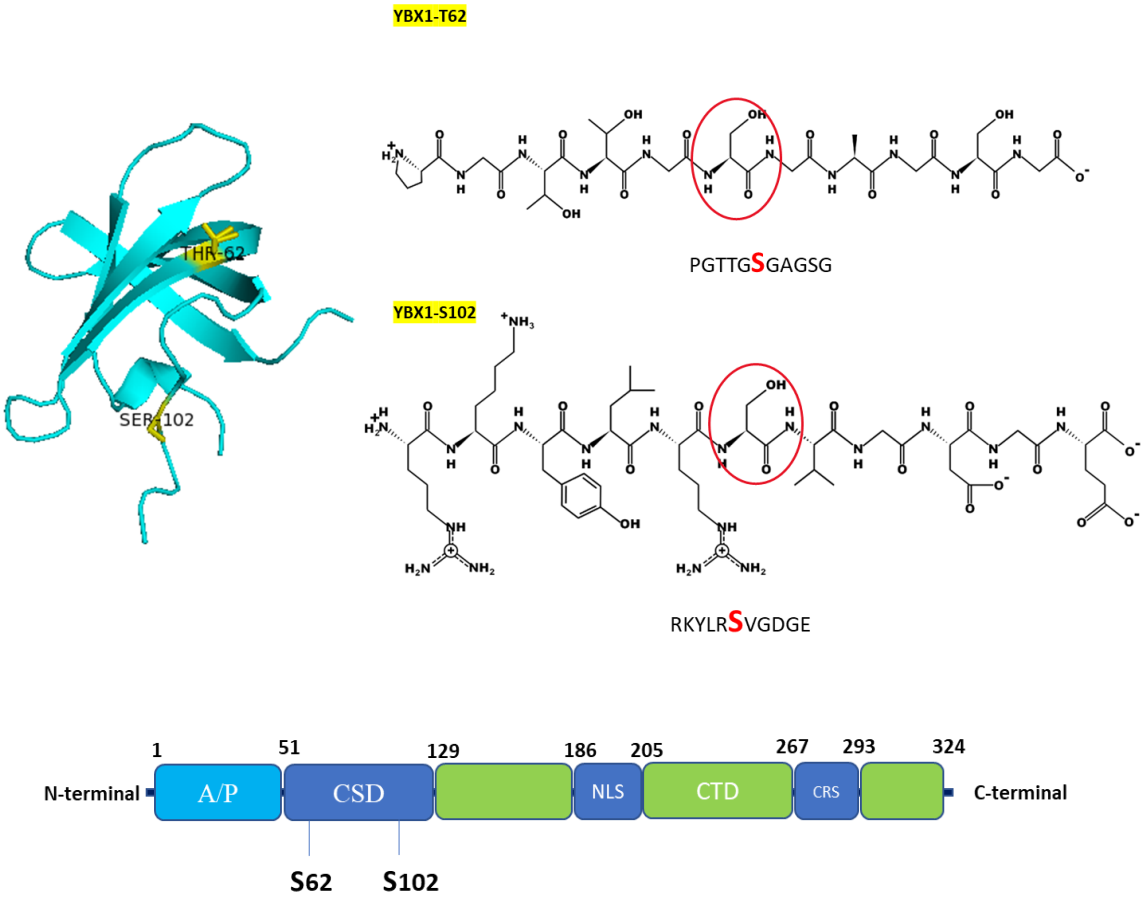

Figure 4.22 The identification of YBX1 phosphorylation sites by AURKA. (Top) A crystal structure of the YBX1-CSD domain illustrates the identified phosphorylation sites Ser62 and Ser102, as well as their localization in the CSD domain. (Right side) is the amino-acid sequence recognized by AURKA, where the residue following the site of phosphorylation is hydrophobic. The phosphorylation sites of YBX1 by AURKA are circled.

4.3 Material and Methods

4.3.1 Cloning and site-directed mutagenesis

YBX1 was cloned into the TAT-HA vector at the BamHI and XhoI sites, noting that all YBX1 mutants were generated using site-directed mutagenesis.

4.3.2 PCR primers

All primers were ordered from Sigma Genosys. See Chapter 5, Table 2, for primer sequences.

4.3.3 Transformation and production of plasmid DNA

See the methodology chapter, Chapter 5.

4.3.4 Bacterial protein expression and purification

The cloned 6x-His-YBX1 was expressed in BL21 *E. coli* competent cells and purified using a French press machine and Ni-NTA beads. YBX1 were expressed in BL21 competent cells and were confirmed using YBX1 monoclonal antibodies. For more details, see Chapter 5.

4.3.5 Buffers

Most of the buffers used in these experiments (including the protein and kinase lysis buffers, DNA and protein purification buffers, kinase buffers etc.) were made in our laboratory. For more information, see buffer recipes in Chapter 5.

4.4 References

1. Kivinummi, K.; Urbanucci, A.; Leinonen, K.; Tammela, T. L. J.; Annala, M.; Isaacs, W. B.; Bova, G. S.; Nykter, M.; Visakorpi, T., The expression of AURKA is androgen regulated in castration-resistant prostate cancer. Sci Rep 2017, 7 (1), 17978.

2. Sardon, T.; Pache, R. A.; Stein, A.; Molina, H.; Vernos, I.; Aloy, P., Uncovering new substrates for Aurora A kinase. EMBO Rep 2010, 11 (12), 977-84.

3. Prabhu, L.; Mundade, R.; Wang, B.; Wei, H.; Hartley, A. V.; Martin, M.; McElyea, K.; Temm, C. J.; Sandusky, G.; Liu, Y.; Lu, T., Critical role of phosphorylation of serine 165 of YBX1 on the activation of NF-κB in colon cancer. Oncotarget 2015, 6 (30), 29396-412.

4. Matsumoto, K.; Bay, B. H., Significance of the Y-box proteins in human cancers. J Mol Genet Med 2005, 1 (1), 11-7.

5. Skabkin, M. A.; Liabin, D. N.; Ovchinnikov, L. P., [Nonspecific and specific interaction of Y-box binding protein 1 (YB-1) with mRNA and posttranscriptional regulation of protein synthesis in animal cells]. Mol Biol (Mosk) 2006, 40 (4), 620-33.

6. Kretov, D. A.; Clément, M. J.; Lambert, G.; Durand, D.; Lyabin, D. N.; Bollot, G.; Bauvais, C.; Samsonova, A.; Budkina, K.; Maroun, R. C.; Hamon, L.; Bouhss, A.; Lescop, E.; Toma, F.; Curmi, P. A.; Maucuer, A.; Ovchinnikov, L. P.; Pastré, D., YB-1, an abundant core mRNA-binding protein, has the capacity to form an RNA nucleoprotein filament: a structural analysis. Nucleic Acids Res 2019.

7. Kljashtorny, V.; Nikonov, S.; Ovchinnikov, L.; Lyabin, D.; Vodovar, N.; Curmi, P.; Manivet, P., The Cold Shock Domain of YB-1 Segregates RNA from DNA by Non-Bonded Interactions. PLoS One 2015, 10 (7), e0130318.

8. Brent, W. S.; Jill, K.; Joyce, W.; Cathy, L.; Maggie, C. U. C.; Erika, Y.; Dmitry, T.; Shoukat, D.; Colleen, N.; Michael, P.; Grimes, H. L.; Kathy, M.; Sunil, B.; David, H.; Blake-Gilks, C.; Min, C.; Catherine, J. P.; Sandra, E. D., Akt phosphorylates the Y-box binding protein 1 at Ser102 located in the cold shock domain and affects the anchorage-independent growth of breast cancer cells. Oncogene 2005, 24 (26), 4281.

9. Prabhu, L.; Hartley, A. V.; Martin, M.; Warsame, F.; Sun, E.; Lu, T., Role of post-translational modification of the Y box binding protein 1 in human cancers. Genes Dis 2015, 2 (3), 240-246.

10. Kloks, C. P.; Spronk, C. A.; Lasonder, E.; Hoffmann, A.; Vuister, G. W.; Grzesiek, S.; Hilbers, C. W., The solution structure and DNA-binding properties of

the cold-shock domain of the human Y-box protein YB-1. J Mol Biol 2002, 316 (2), 317-26.

11. Ferrari, S.; Marin, O.; Pagano, M. A.; Meggio, F.; Hess, D.; El-Shemerly, M.; Krystyniak, A.; Pinna, L. A., Aurora-A site specificity: a study with synthetic peptide substrates. Biochem J 2005, 390 (Pt 1), 293-302.

CHAPTER 5. METHODOLOGY

5.1 Cloning and Site-Directed Mutagenesis

SPOP and YBX1 and their mutants were cloned into the TAT-HA vector at the BamHI and XhoI sites. Primer sequences shown in **Table 5.1** were designed by Dr. Shah and ordered from SigmaGenosys. SPOP and YBX1 mutants were generated using site directed mutagenesis. Two PCR fragments were generated and overlapped using the annealing temperature recommended by SnapGene software. The digested products − digested using BamHI/Xho1 restricting enzymes − were then ligated to the TAT-HA vector. The generated plasmids were then transformed using DH5α competent E.Coli cells. Positive colonies were transformed in BL21 E.Coli cells for protein production (Figure 5.1).

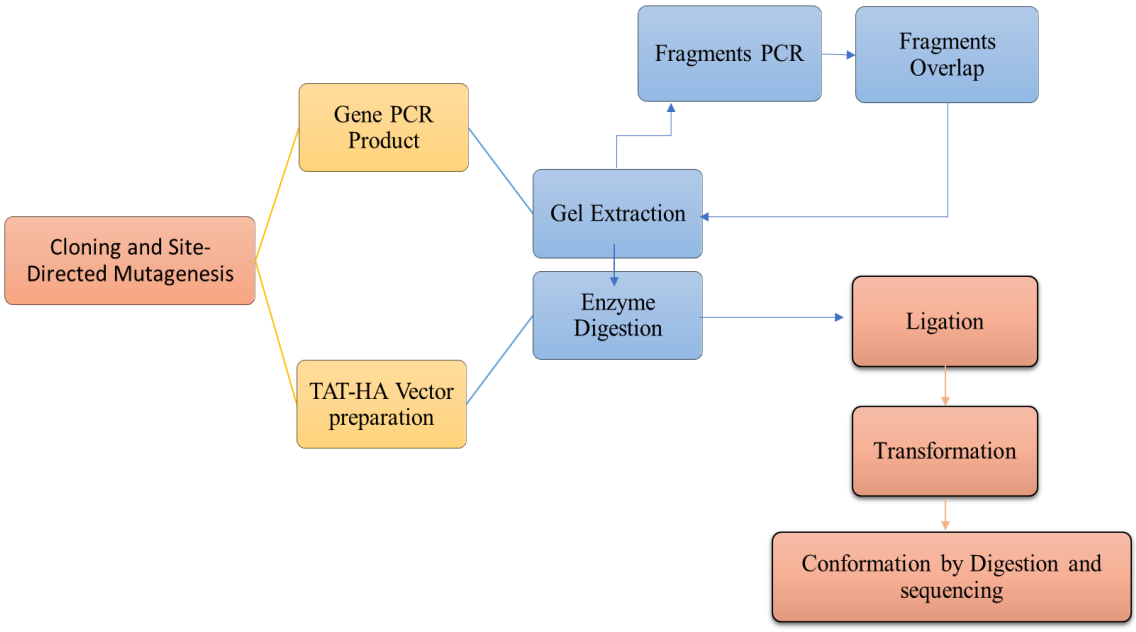

Figure 5.23 Step flow-chart overview of cloning and site directed mutagenesis.

Table 5.1: List of SPOP primers

Note	Primers	Sequences
Wild type	**SPOP-BamHI-1**	GCTGGATCCATGTCAAGGGTTCCAAGTCCT
	SPOP-HA-Xho1-2	TACAGTCTCGAGTTAAGCGTAATCTGGAACATCGTATGGGTA GGATTGCTTCAGGCGTTTGCG
	SPOP-180-R1-2	AGTGAATTCTTACTTTACCATGTTCATGG
Truncated SPOP	SPOP-181-BamHI-1	GCTGGATCCATGGTTCCTGAGTGCCGG
	SPOP-300-Xho1-2	TACAGTCTCGAGTTACTCCACGGACAGGTTAC
	SPOP-301-BamHI-1	GCTGGATCCATGCGCTTAAAGGTCATGTG
LIMK2 sites	SPOP-SS59-A1	ATTAAAAGTTCTACATTTGCAGCAGGAGCAAATGATAAACTG
	SPOP-SS59-A2	CAGTTTATCATTTGCTCCTGCTGCAAATGTAGAACTTTTAAT
	SPOP-S59-A1	AGTTCTACATTTTCAGCAGGAGCAAATGATAAA
	SPOP-S59-A2	TTTATCATTTGCTCCTGCTGAAAATGTAGAACT
	SPOP-S226A-1	CGTTCTCCGGTTTTTGCTGCCATGTTTGAACATGAAATG
	SPOP-S226A-2	CATTTCATGTTCAAACATGGCAGCAAAAACCGGAGAACG
	SPOP-S171A-1	CAAGATTCTGTCAACATTGCTGGCCAGAATACCATGAAC
	SPOP-S171A-2	GTTCATGGTATTCTGGCCAGCAATGTTGACAGAATCTTG
	SPOP-S33A1	ATCAAGGTAGTGAAATTCGCCTACATGTGGACCATCAAT
	SPOP-S33A2	ATTGATGGTCCACATGTAGGCGAATTTCACTACCTTGAT
AURKA sites	SPOP-T56A1	GAAGTCATTAAAAGTTCTGCATTTTCATCAGGAGCAAAT
	SPOP-T56A2	ATTTGCTCCTGATGAAAATGCAGAACTTTTAATGACTTC
	SPOP-S105A1	CGGGCAAAATTCAAATTCGCCATCCTGAATGCCAAGGGA
	SPOP-S105A2	TCCCTTGGCATTCAGGATGGCGAATTTGAATTTTGCCCG

Table 5.2: List of YBX1 primers

Note	Primers	Sequences
Wild type	**YB1-BamHI-1**	GCTGGATCCATGAGCAGCGAGGCCGAG
	YB1-HA-Xho1-2	TACAGTCTCGAGTTAAGCGTAATCTGGAACATCGTATGGGTACTC AGCCCCGCCCTGCTC
Truncated YBX1	YBX1-130-R1-2	AGTGAATTCTTAAACACCACCAGGACC
	YBX1-124-BamHI-1	GCTGGATCCATGAATGTTACAGGTCCTGG
Aurora-A sites	YBX1-T62A1	GCAACGAAGGTTTTGGGAGCAGTAAAATGGTTCAATGTA
	YBX1-T62A2	TACATTGAACCATTTTACTGCTCCCAAAACCTTCGTTGC
	YBX1-S102A1	CCCAGGAAGTACCTTCGCGCTGTAGGAGATGGAGAGACT
	YBX1-S102A2	AGTCTCTCCATCTCCTACAGCGCGAAGGTACTTCCTGGG

5.2 Competent cells preparation

A sample of DH5α and BL21 DE3 competent cells were kindly given to us by Dr. Chittaranjan Das's group. The cells were then streaked on an LB agar plate without carbenicillin and prepared using the inoue method.

5.3 Sf9 cell protein expression and purification

AURKA and LIMK2 kinases were expressed in Sf9 cells by Nikhil Kumar and Keith Viccaro and and stored at -20°C. The Pellets were thawed on ice for 10-15mins and resuspended in a 5mL kinase lysis buffer (Table 5.2) with freshly added 1mM PMSF.

5.4 Transformation and production of plasmid DNA

Under sterile conditions and a clean environment, the competent cells were placed on ice to thaw gently before being inoculated with the cloned plasmid using a 1mL Eppendorf tube. Based on the plasmid DNA concentration, the cells were inoculated with 1-5μL DNA.

They were then kept on ice for 30 minutes. During this time, the water bath was set up at 42°C. The inoculated cells were heat-shocked for 45-60 minutes and placed on ice immediately for 3 minutes. At this point, 900μL of a sterile and fresh LB broth media were added to the cells and incubated for 1 hour, at 37°C. The cells were then spun down at 6000 rpm for 2 minutes and plated on LB agar plates containing 100μg/mL carbenicillin. The plates were incubated at 37°C overnight.

The same transformation procedure was used for both types of competent cells. DH5α cells were used to produce the plasmid DNA in general, and in the ligation process to produce the new clone. This protocol differs only when growing cells from a plate. If the transformation is for general DNA production of a known DNA, then a swipe of colonies can be cultured in a 30mL scale and miniprepped for purification. If the transformation is for a ligated plasmid to check for positive colonies, then individual colonies will be selected carefully and grown separately in small cultures. Miniprep and DNA digestion with specific enzymes will then be used to test for positive colonies. However, if the transformation is for protein expression, the same procedure will be used, followed with the bacterial protein expression and purification protocol.

5.5 Bacterial 6-His-tagged Protein Expression

6x-His tagged proteins were expressed using BL21 *E. coli* competent cells and purified using Ni-NTA beads. A freshly transformed plate was used to inculcate a 30mL starter culture containing 30mL of sterile and fresh LB media, plus 100μg/mL of Carbenicillin. The starter culture was grown at 37°C, 200rpm overnight, and then spun down and washed 2-3 times with fresh media before being added to a 600mL culture media supplemented

with 100μg/mL of Carbenicillin. The large culture was grown until the optical density OD600 reached 0.4-0.8, a range that depended on the expression level of the protein. 100 μM Isopropyl β-D-1-thiogalactopyranoside (IPTG) was added after the culture cooled down to room temperature (RT) and left to express the protein overnight-RT*. The culture was then spun down and the pellets were frozen at -20°C, then purified the next day or kept until needed.

* Note: Some proteins might require different expression conditions. We had to test the expression of the protein on a small scale to optimize the conditions, such as expression duration time, temperatures, IPTG concentration, and soluble vs. insoluble protein.

5.6 Bacterial 6-His-tagged protein purification

Pellets were thawed on ice for 1 hour and resuspended in 10mL of protein lysis buffer (see section 5.9) with freshly added 1mM phenylmethane sulfonyl fluoride (PMSF). Three cycles were enough to lyse the cells efficiently. The lysates were centrifuged at 10000rpm for 20 minutes at 4°C and the supernatant was collected in a 15mL falcon tube. 100 μL of Ni-NTA agarose beads (from GoldBio technology) were washed once with water and then twice with a lysis buffer, then added to the cleared lysate. The suspension was installed to rotate on the end-over-end shaker at 4°C for 1-2 hours. After 1 hour, the beads were centrifuged at 10000 rpm for 1 minute at 4°C. Bead color can be a good indicator of how much protein has bound to it and can be monitored during wash times to help with efficient washes. Three types of washing buffers were used to purify the protein: low, medium and high buffers (see Table 5.2). The beads were washed 3 times with 1mL of low buffer, 2 times with 1mL of medium buffer, and 1 time with 1mL of high buffer. In between each wash, the tube was changed to increase the purity of the proteins. The proteins were then

eluted using an elution buffer (see Table 5.2), and 3-5 100μL fractions of each were collected. The beads were saved in the 100μL elution buffer until we checked that the proteins were eluted successfully. The purified proteins were then confirmed by size using sodium dodecyl sulfate (SDS) polyacrylamide gel electrophoresis, stained with Coomassie stain. The proteins were identified through western blot using antibodies specific for each protein. SPOP, YB1, LIMK2 and ARK-1 antibodies from Santa Cruz Biotechnology, Inc. were used at a 1:1000 dilution.

5.7 Peptide Assay

The peptide assay was used to check Aurora A and LIMK2 activity, and mainly for Aurora A kinase activity to determine the optimal concentration of TPX2 that should be used for maximum enzyme activity. The kinase was used after purification and elution from the Ni-NTA beads to set up the peptide/Kinase reaction. See section 1.8 for the kinase purification procedure.

5.8 Kinase Assays

5.8.1 Preparing and purifying the kinase

A pellet of SF9 cells that expressed LIMK2/AURKA and had been stored at -20°C was thawed in ice. The cells were then lysed with kinase lyses buffer with a pH=8 (see section 5.9) with freshly added 1mM PMSF. The amount of lysis buffer used was 5mL for 1 pellet (cells were spun down from a 50mL sf9 cell culture). The cells in lysis buffer were left in ice for 30 minutes and gently inverted every 10 minutes. The lysed cells were spun down again at 10000 rpm for 20 minutes at 4°C. During this time, 60μL of Ni-NTA beads were washed once with 1mL sterile diH_2O and twice with low buffer or kinase lysis buffer. Then

the supernatant/lysate was collected in a 15mL falcon tube and mixed with the washed beads. The suspension was installed to rotate on the shaker/rotator at 4°C for 1 hour. Next, the beads that bound to the kinase were centrifuged at 10000 rpm for 1 minute at 4°C and transferred to a 1.5mL Eppendorf tube. The beads were washed 3 times with low buffer and 2 times with medium buffer and 1 time with high buffer, then 1 time with a 1X kinase buffer (see Table 5.2). After the last wash with the 1X kinase buffer and spinning down the beads after each wash, as much kinase buffer as possible was removed while being careful not to remove any of the beads, and a 100μML of fresh 1X kinase buffer was added to the beads to prepare for the (nonradioactive) cold ATP reaction.

5.8.2 Cold ATP reaction

The kinase was run in a nonradioactive ATP reaction for 2 hours to reduce the nonspecific phosphorylation background and the autophosphorylation. To the100μML bead solution, 1mM of cold ATP and 15mM $MgCl_2$ were added. The reaction pre-incubated on the shaker for 2 hours at room temperature (RT). Since there was a chance that the kinase might be released from the beads at RT, 1 mL of 1X kinase buffer was added to the reaction and left on the rotator for 1 hour to make sure the kinase bound to the beads. Next, the beads were spun down at 10000rpm for 1 minute and the reaction solution was removed. In this stage, the beads had to be washed 3 to 4 times to remove the cold ATP before the actual kinase assay.

5.8.3 Sample preparation

Mainly the reaction samples contained the kinase, the substrate/protein, and the radio labeled [γ-32P] ATP. Table 5.3 shows the general setup for kinase assay samples. The sample reactions were done in a 1.5 Eppendorf tube, where water was added first, then the

10X kinase buffer (10X K.B), the substrate, and the kinase, followed by the ATP which was added last. After 30 minutes, the reactions were stopped upon the addition of SDS loading dye and heated for 3-5 minutes at 100°C and then separated by SDS-PAGE gel. LIMK2 kinase was best detected with Coomassie stained gel, but AURKA was not detected with Ponceau S or Coomassie. Because of that, the gel was either exposed for autoradiography directly after fixation for 30 minutes or transferred to a polyvinylidene difluoride (PVDF) membrane, and then exposed for autoradiography.

Table 5.3: General sample preparation for kinase assay

Sample	Substrate	Kinase	10X K.B	[γ-32P] ATP	H2O	Elution Buffer
1. Kinase alone	0	5	2.5	0.5 µCi	Depends on the final scale	
2. Substrate + Kinase	vary	5	2.5	0.5 µCi	Depends on the final scale	
3. Substrate alone	vary	0	2.5	0.5 µCi	Depends on the final scale	

5.9 Buffers and solution recipes

5.9.1 Buffers for purifying plasmid DNA

P1 resuspension buffer	50 mM Tris HCl pH 8.0, 10 mM EDTA, 100 µg/ml RNase A 6.1 g Tris, 3.7 g EDTA, 10 µg/mL RNase
P2 lysis buffer	200 mM NaOH, 1% SDS 8.0 g NaOH, 100 ml of 10 % SDS ddH2O to a final volume of 1L
N3 neutralization buffer	4.2 M Gu-HCL, 0.9 M Potassium Acetate pH=4.8
PE washing buffer	10 mM Tris HCL pH 8.5 and 80% Ethanol

5.9.2 Buffers for DNA agarose gel

TAE	40 mM Tris-acetate, 1 mM EDTA 50% TAE: 242g Tris, 57.1 glacial acetic acid, 100mL pH=8 EDTA and ddH2O to a final volume of 1L
1% DNA agarose gel	50mL TAE, 0.5g agarose DNA mixed and microwaved, add 1µL ethidium bromide EtBr after it cools down The percentage of the agarose was determined based on the DNA size

5.9.3 Buffers for Protein Purification

Protein lysis buffer	50 mM Tris pH 8.00, 500 mM NaCl, 1% NP-40, 5-10% glycerol
Low washing buffer	50 mM Tris pH 8.00 and 150 mM NaCl
Med washing buffer	50 mM Tris pH 8.00, 150 mM NaCl, and 10 mM imidazole
High washing buffer	50 mM Tris pH 8.00, 150 mM NaCl, and 20-50 mM imidazole
Elution buffer	50 mM Tris pH 8.00, 50 mM NaCl, and 250 mM imidazole

5.9.4 Buffers for western blot and protein staining

SDS-PAGE running buffer	25 mM Tris, 192 mM glycine, 0.1% SDS 3g Tris, 14.4 glycine, 1g SDS and ddH2O to a final volume of 1L
Western blot - Transfer buffer	25 mM Tris, 192 mM glycine, 10% methanol 3g Tris, 14.4 glycine, 100mL methanol and ddH2O to a final volume of 1L
TBS buffer	25 mM Tris, 150 mM NaCl, 2 mM KCl, pH 7.5 3g Tris, 8g NaCl, 0.2g KCl and ddH2O to a final volume of 1L
TBST buffer	1L TBS buffer + 1mL Tween-20
Coomassie stain	0.1% Coomassie R250, 10% acetic acid, 40% methanol
Coomassie de-stain	20% methanol, 10% acetic acid
Ponceau stain	1g Ponceau, 50mL acetic acid and ddH2O to a final volume of 1L
SDS- protein gel 10%:	12.6 mL ddH2O, 10.66 mL 30% Acrylamide, 8mL 1.5M Tris pH 8.8, 320 µL 10 % SDS, 320 µL 10 % APS, 32 µL TEMED
Stacking gel 6%	10.6 mL ddH2O, 4 mL 30% Acrylamide, 5 mL 0.5M Tris pH 6.8, 200 µL 10% SDS, 200 µL 10% APS, 20 µL TEMED